

## **Development and Investigation of Communication Issues on a CubeSat-onboard Amateur Radio Payload with APRS Digipeater and Store-and-Forward Capabilities**

Adrian C. SALCES<sup>1,\*†</sup>, Marloun P. SEJERA<sup>1</sup>, Sangkyun KIM<sup>1</sup>, Hirokazu MASUI<sup>1</sup>, Mengu CHO<sup>1</sup>

<sup>1</sup> Laboratory of Lean Satellite Enterprises and In-orbit Experiments, Kyushu Institute of Technology,  
1-1 Sensui-cho, Tobata-ku, Kitakyushu City 804-8550, Japan

### SUMMARY

Automatic Packet Reporting System (APRS) is originally a terrestrial packet communication system widely utilized by amateur radio stations to exchange various information. To extend this capability over a geographically broad coverage, a few microsatellites previously carried an APRS digipeater payload for global amateur community use, and then there have been proposals to do this on smaller nanosatellite platforms, such as the CubeSat. Although CubeSat is an attractive platform for this application – due to its substantially simpler design, lower cost, and faster development time – it also presents several technical challenges such as tight space, power, and communication link budgets. In this paper, we discuss the design, development and testing of an amateur radio payload that operates in the 145.825 MHz amateur frequency, consists of mostly commercial-of-the-shelf components and supports both APRS digipeater and store-and-forward (S&F) communication for remote data collection. The payload was carried as a technology demonstration mission of a 1U CubeSat constellation developed at the Kyushu Institute of Technology under the BIRDS-2 Project. Several amateur operators confirmed reception of the payload's beacon message but full two-way communication failed due to uplink communication problems. This paper also tackles the investigation on the causes of failure through ground-based communication tests, as well as the recommendations from the findings.

**KEY WORDS:** CubeSat; APRS; store-and-forward; remote data collection; amateur radio

---

\* Corresponding author. Adrian C. SALCES.

† E-mail: [q595906k@mail.kyutech.jp](mailto:q595906k@mail.kyutech.jp).

Received 19<sup>th</sup> February, Revised 12<sup>th</sup> May, Accepted 6<sup>th</sup> June.

**ACRONYMS/ABBREVIATIONS**

ACK – acknowledgment  
ADCS – attitude determination and control subsystem  
AFSK/FM – audio-frequency shift keying on frequency modulation  
APRS – Automatic Packet Reporting System  
APRS-DP – Automatic Packet Reporting System Digipeater  
AT – Acceptance Test  
AUT – Antenna under test  
BER – bit error rate  
bps – bits per second  
COM – Communication Subsystem  
COTS – commercial-off-the-shelf  
CW – continuous wave  
EM – Engineering Model  
EMI – electromagnetic interference  
EPS – electric power subsystem  
FAB – Front Access Board  
FAC – Full anechoic chamber  
FCS – frame check sequence  
FM – Flight Model  
FT – Functional Test  
GMSK – Gaussian minimum shift keying (modulation)  
GPS – Global Positioning System  
GS – Ground Station  
GST – ground sensor terminal  
IMN – impedance matching network  
ISS – International Space Station  
JAXA – Japan Space Exploration Agency  
KISS – Keep It Simple, Stupid (protocol)  
LEO – Low-Earth orbit  
MCDM – mission control and data management  
MCC – mission control center  
MCU – microcontroller unit  
OBC – On Board Computer  
PC – Personal Computer  
PCB – Printed Circuit Board  
QT – Qualification Test  
RAB – Rear Access Board  
RDCS – remote data collection system  
RF – radio-frequency  
RSSI – received signal strength indicator  
RTC – real-time clock  
SPI – Serial Peripheral Interface  
SNR – signal-to-noise ratio  
S&F – store-and-forward  
TNC – terminal node controller  
TLE – two-line elements  
UART – Universal Asynchronous Receiver-Transmitter  
TVT – Thermal Vacuum Test  
TRX – transceiver  
UART – Universal Asynchronous Receiver-Transmitter  
UHF – Ultra High Frequency (specifically 430-440 MHz amateur band)  
UTC – Coordinated Universal Time  
VHF – Very High Frequency (specifically 144-146 MHz amateur band)  
1U//2U/3U – One-unit/two-unit/three-unit (CubeSat)

## 1. INTRODUCTION

The LEO microsattellites developed in the 1980s and 1990s by research and amateur radio organizations have demonstrated their use as relatively simple and low-cost space-based asset for remote data collection and messaging [1][2]. Following these, since 2000s, a few satellites (mostly non-CubeSats ranging from 10kg to 70kg) have carried an Automatic Packet Reporting System (APRS) digipeater payload for global amateur community use, including the Amateur Radio on the ISS (ARISS), PCSAT [3], LAPAN-A2 [4], Diwata-2 [5]. APRS originated as a terrestrial amateur radio-based real-time packet communication protocol that enabled operators to exchange various situational information in their local area (e.g., weather reporting, object/vehicle position tracking, messaging and emergency response). Later on, with stations having been interconnected by the Internet (called IGates) through the APRS Global Internet System (APRS-IS), global monitoring of local activities and two-way end-to-end messaging between any two APRS users have been supported [6]. Due to a satellite's capability to provide a geographically broad coverage directly below its moving footprint, an APRS digipeater (APRS-DP) onboard a satellite would subsequently play a significant role of covering remote areas not reached by terrestrial means.

More recently, with the rise of even smaller classes of satellite, less than 10kg, especially the standardized CubeSat [7] platforms, there have also been proposals and actual implementations of CubeSats carrying an APRS-DP. These include, among others, PSAT-1 (1.5U, 2015), PSAT-2 and BRICSAT-2 (1.5U, 2019), and the three BIRDS-2 CubeSats (1U, 2018). The idea proposed in [8] is for these and future APRS-DP satellites in orbit to share a common channel (145.825 MHz) and a generic digipeater alias (APRSAT and ARISS) to accumulate all user traffic on an Internet server, hence integrating all worldwide users and ground stations.

Besides APRS-DP, which relays packets in nearly real-time fashion, there have also been an increasing interest to utilize CubeSats and pico/nanosatellites for more delay-tolerant store-and-forward (S&F) type of communication for remote data collection. A S&F CubeSat constellation, for example, can be launched at a still relatively low cost to serve their potentially niche practical application as relay nodes for collecting data from environmental/weather/scientific sensing stations deployed in remote or isolated sites – those usually not served by regular communication infrastructure or where direct access is very challenging. Since many of these scenarios also involve low-volume data and high latency is tolerable, a S&F CubeSat constellation can be considered as a practically suitable solution. Several previous publications [9]-[15] have dealt mainly with the concept and analysis of S&F nanosatellite-enabled remote data collection systems. A few works [16]-[18] have demonstrated this capability for CubeSats through actual implementations but significant contributions on this topic can still be done, especially on discussion of results and experiences gained from development of an actual system. While employing CubeSats for the above-mentioned communication purposes is attractive because of their simpler architecture, shorter development time and lower cost, enabling this idea requires dealing with tight design constraints on space, power and communication link budget.

With the aim to explore using CubeSats for the complementary applications of APRS-DP and S&F communication for remote data collection in the amateur band, the BIRDS-2 Project team at the Kyushu Institute of Technology (Kyutech) developed an amateur radio payload having both communication capabilities. The payload was carried onboard the 1U CubeSat constellation of the BIRDS-2 Project (namely, BHUTAN-1 of Bhutan, MAYA-1 of the Philippines and UiTMSAT-1 of Malaysia). It was developed and integrated to the satellites within a 15-month time frame from December 2016 to February 2018 – about 11 months for engineering model and four months for final assembly, integration and test of flight models. To lower the cost and make the system easily available for use by the global amateur community, the CubeSat-onboard payload, ground sensor terminals (GST) that send data to the payload and APRS user radios all operate in half-duplex mode in the 145.825 MHz amateur radio frequency (like in [13][14]). The CubeSats were deployed from the ISS on August 2018 and then the amateur radio payloads operated for about a year and three months before being deactivated.

The purpose of the present paper is to explain the design, development and testing of the APRS-DP/S&F mission payload onboard the BIRDS-2 Project's 1U CubeSat constellation. Initial part of this work was presented in a conference paper [19]. Several amateur operators around the globe confirmed reception of the

payload's regular beacon message but full two-way communication failed due to uplink communication problems. The causes of failure were investigated through ground-based communication tests. The findings and lessons learned from the investigation, as well as the recommended design improvements are also tackled in this paper. The design recommendations have been considered for implementation in the succeeding BIRDS-4 Project at Kyutech and the BIRDS-2S Project at the University of the Philippines-Diliman (UPD). Three BIRDS-4 and two first batch BIRDS-2S 1U CubeSats are expected to be deployed from ISS on summer 2020 and fall or later 2020, respectively. By sharing their recent work with this paper, the authors aim to contribute to the growing interest of utilizing CubeSats for providing space-based data communication capabilities.

This paper comprises of five sections. The second section describes the system architecture, payload design and development, system level integration and space environment tests. The third section tackles the investigation on uplink communication failure and ground-based communication tests. The fourth section provides the lessons learned and recommendations from the investigation and the final section gives the conclusions.

## 2. SYSTEM ARCHITECTURE, PAYLOAD DESIGN, DEVELOPMENT, INTEGRATION AND TESTS

### 2.1. System Architecture

The APRS-DP/S&F mission payload onboard the BIRDS-2 CubeSat constellation provides both APRS-DP and S&F communication capabilities using a common hardware and amateur radio frequency of 145.825 MHz. The APRS-DP mission supports real-time packet (message, position, beacon, telemetry, etc.) repeating between amateur radios and stations located on the same footprint, as illustrated in Figure 1. The satellite-based APRS-DPs of the BIRDS-2 constellation were aimed to complement the existing terrestrial APRS network, as well as an addition to other APRS satellites previously launched into orbit. Using an APRS-capable radio, a "ham" sends an APRS message or packet to the satellite and then the payload retransmits it immediately, allowing other hams or amateur stations to receive it.

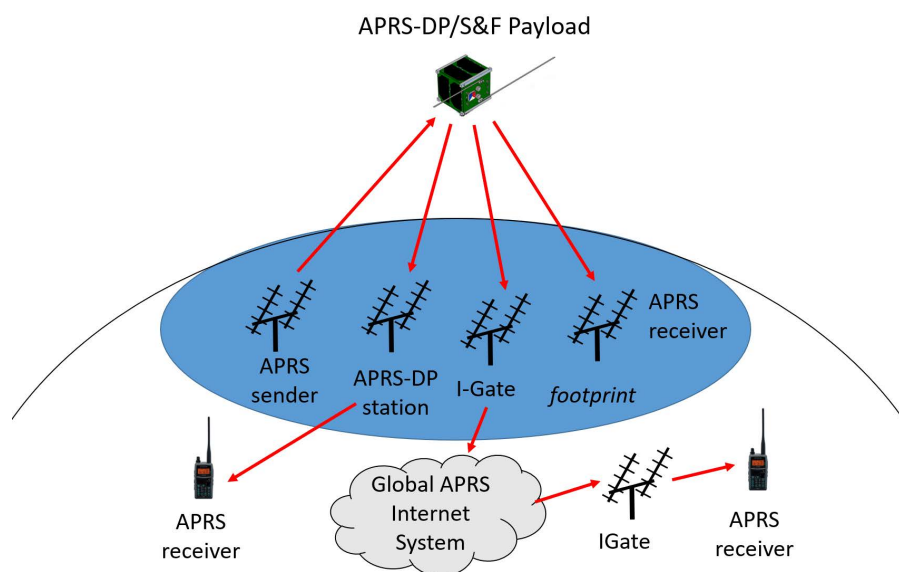


**Figure 1 Conceptual operation of the APRS-DP mission**

On the other hand, the system architecture of the BIRDS-2 S&F CubeSat constellation-based remote data collection system (RDCS) is given in Figure 2. It consists of three main segments: (1) Ground Sensor Terminal (GST) Segment, (2) CubeSat-onboard S&F Payload (“Payload”) Segment, and (3) Mission Control and Data Management (MCDM) Segment. Each GST consists of one or more sensors, a microcontroller unit (MCU), a VHF half-duplex transceiver, an antenna with rotator (for satellite tracking) mounted on a mast, and solar-battery power system for autonomous operation. In “store” phase, the payload receives sensor packet from any GST that transmits during satellite pass and saves them in an onboard flash memory. In “forward” phase, after receiving an uplink command, gathered data are downloaded to a BIRDS ground station. Downloaded data are transferred to an online storage, processed at the mission control center and distributed to data users. Mission operation control, data download, storage, processing, and distribution to users are handled by the MCDM. By employing a CubeSat constellation, the upload data throughput will be roughly a multiple of that of single CubeSat case. Also, by using a network of ground stations, more data download flexibility and frequency can be achieved. The onboard payload, GSTs and handheld radios operate in the VHF amateur radio band at 145.825 MHz to achieve a low cost system that is easily available for use by the amateur community (like in [13][14]).

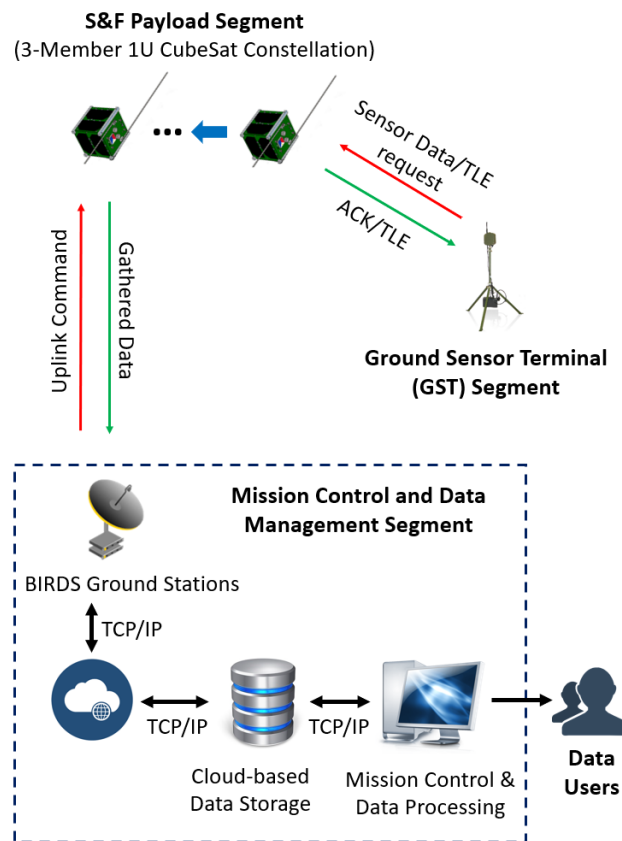


**Figure 2 System architecture of the BIRDS-2 S&F CubeSat constellation-based remote data collection system**

## 2.2. Payload Design Considerations and Implementation on the BIRDS-2 CubeSat

When designing the payload, the following factors were considered: (a) utilizing low cost, commercial-off-the-shelf (COTS) components, (b) simple design requiring short development time for hardware and software, (c) having low energy consumption and small form factor so it can be accommodated on a CubeSat. These factors were crucial because the payload had to be accommodated on the BIRDS-2 1U CubeSat that was expected to carry other subsystems and mission payloads sharing in the satellite resources. The payload had to be built, tested and integrated with the satellite within the project’s original development timeline of about

one year and three months, from mission planning to completion of flight models. The use of COTS components was possible due to availability of transceivers and modules supporting the modulation and communication protocol commonly used for amateur radio (in the case of APRS, audio-frequency shift keying on frequency modulation or AFSK/FM and AX.25 link layer protocol). Inexpensive implementations utilizing COTS components have been described in literature, for the S&F nanosatellite [14] and ground terminals [20][21]. In [14], the communication program, modem, packet handling and onboard data handling are handled by one MCU on a single board, and a half-duplex COTS VHF amateur transceiver is used for transmitting and receiving RF signal. This integrated approach results in a more compact onboard system, although it requires more programming work on the part of the developer to implement the APRS application, AX.25 protocol [22], and AFSK modulator/demodulator (modem) on the MCU.

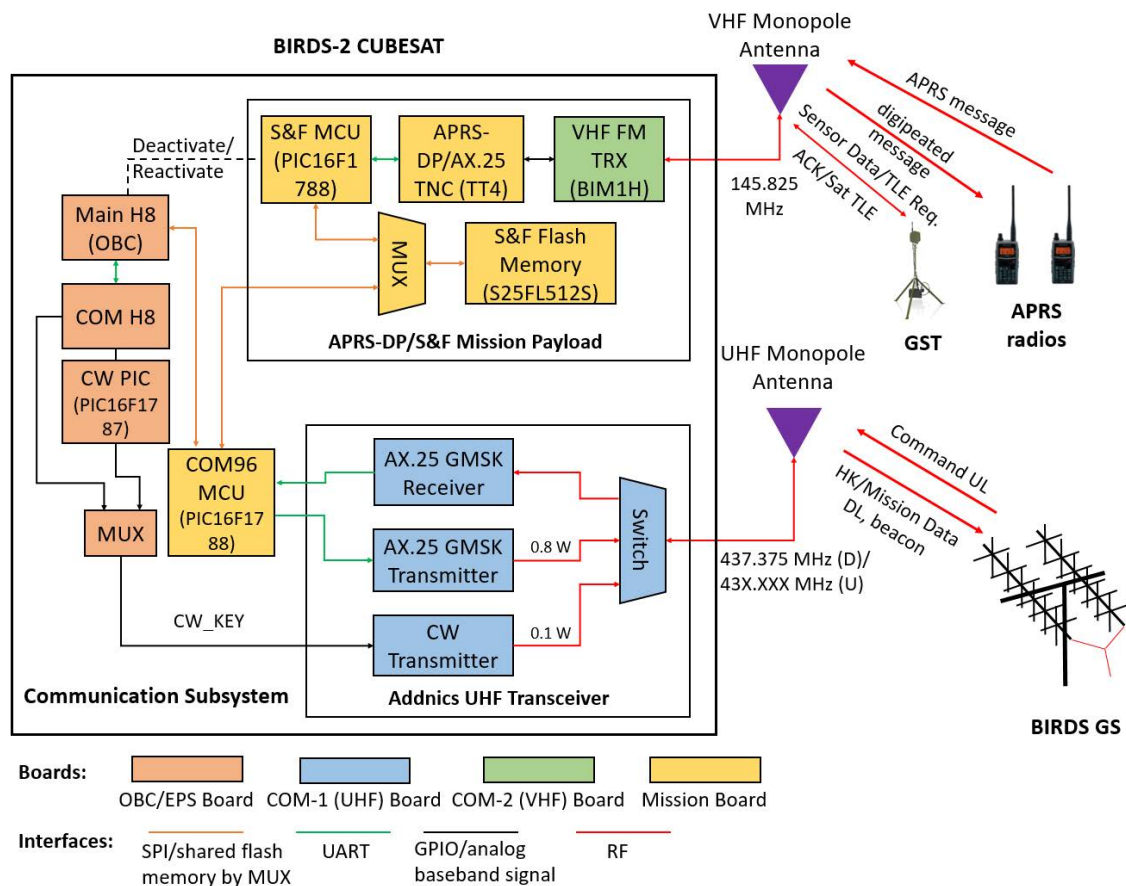


**Figure 3 Block diagram of the BIRDS-2 APRS-DP/S&F payload and communication subsystem**

The block diagram of our own APRS-DP/S&F payload implementation is shown in Figure 3 and the flight model boards are shown in Figure 4. It is made by integrating individual COTS components – including a VHF FM transceiver (Radiometrix’s BIM1H), a stand-alone APRS-DP module (Byonics’ TT4), a MCU running the S&F program (Microchip’s PIC16F1788), a multiplexer (ADI’s ADG774) and a 64-Mbyte flash memory (Cypress’ S25FL512S). Aside from being very low cost, these components were selected based on size, power consumption, ease of interfacing and little programming work required for the development. The VHF transceiver has an output RF power of 0.5 W, dimensions of 33 mm (L) x 23 mm (W) x 12 mm (T) and operates at 145.825 MHz for both uplink and downlink, in half-duplex mode. A VHF monopole antenna with nichrome wire heating deployment mechanism is connected to the VHF transceiver. The TT4 is a stand-alone module providing all necessary functionalities – APRS digipeater, AX.25 protocol terminal node controller (TNC) with

KISS protocol support for UART communication between it and the S&F MCU, and a 1200 bps AFSK modem. Taking advantage of TT4’s features, the developer could focus on rendering the S&F program on the S&F MCU within a short time. The original TT4 package was altered and soldered to the mission board using a customized adaptor board.

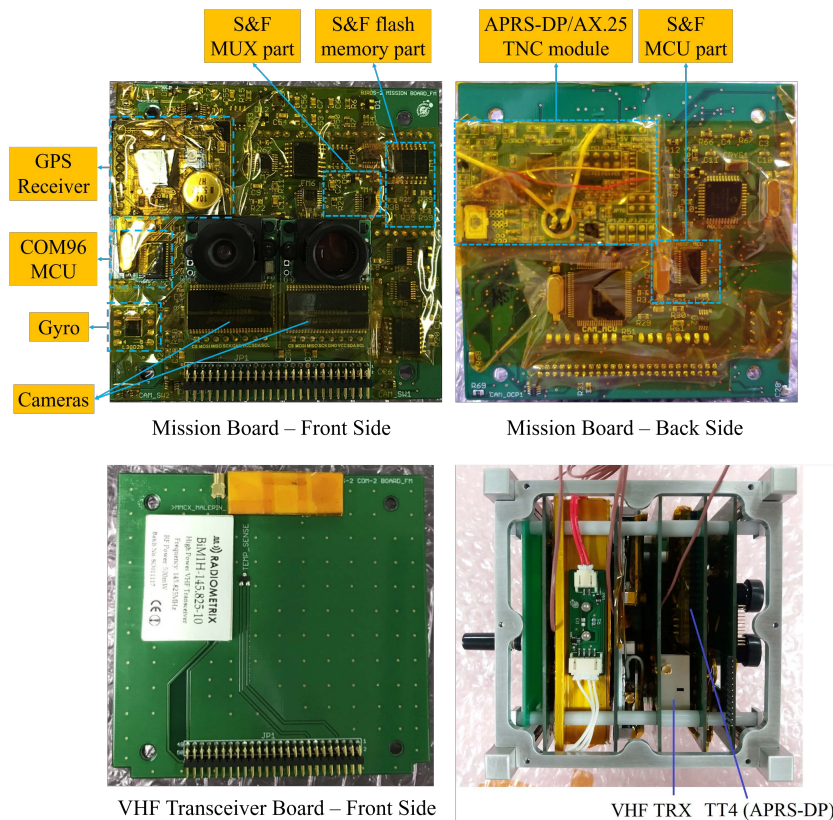


**Figure 4 BIRDS-2 APRS-DP/S&F payload flight model boards: mission board hosting the APRS-DP/TNC module, S&F MCU and flash memory; VHF transceiver board; assembled with other internal boards (lower right)**

The payload directly interacts with the GSTs (or with APRS-DP users’ handheld radios) during the “store” phase. Whenever it receives a valid packet from any GST, it saves the packet in the flash memory and automatically sends an ACK packet. As an added feature, upon receiving a special request packet from any GST to download the two-line elements (TLE), it transmits a packet bearing the satellite’s latest TLE information (which is sent from the command ground station). The S&F MCU runs the S&F program sequence including packet generation (in transmit side) and parsing (in receive side). In reception, it decomposes the packet into separate fields and recognizes the GST’s identification callsign, packet header and footer, packet type and sensor data. In transmission, it does the reverse to compose the appropriate downlink packet to send to the GST. The program flow diagram of the S&F MCU is very simple, as illustrated in Figure 5. The stored data are downloaded to the Mission Control Center (or any BIRDS ground station) through the UHF communication transceiver at the rate of 9600 bps (GMSK modulation, AX.25 protocol). The same UHF transceiver receives uplink command from the ground station, including the commands to download the stored data and to upload the latest satellite TLE.

For better context on how the payload is integrated with the whole satellite, satellite drawings are given in Figure 6. Overall, the components of the payload occupy about ¼ of the space on the mission board (which also hosts ADCS, the COM96 MCU portion of the communication subsystem, and other mission payloads such as camera, GPS receiver, and magnetic field sensor), except for the VHF transceiver that is placed on a separate

board. The payload alone, when powered by a 5V supply, consumes only about 0.29 W while in receive or standby mode and 1.4 W during active RF signal transmission.

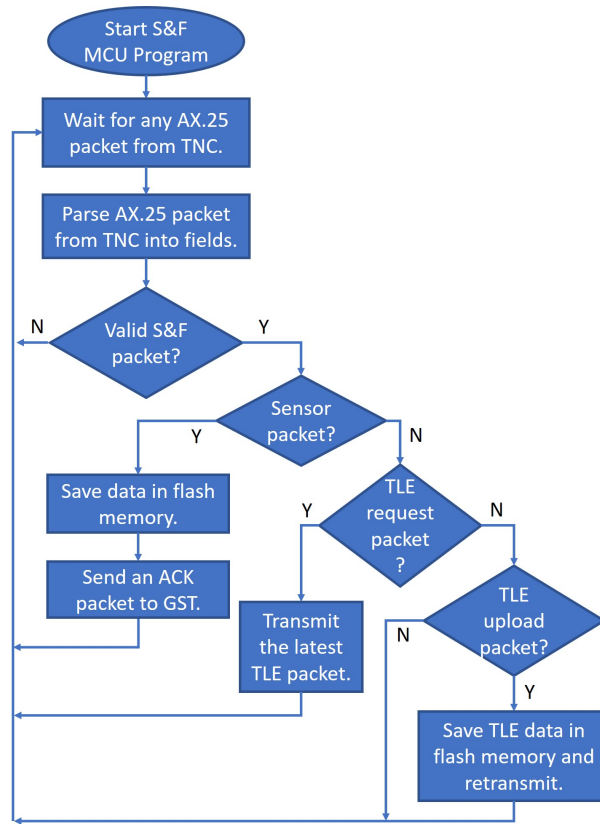


Figure 5 Program flow diagram of the S&F payload’s MCU

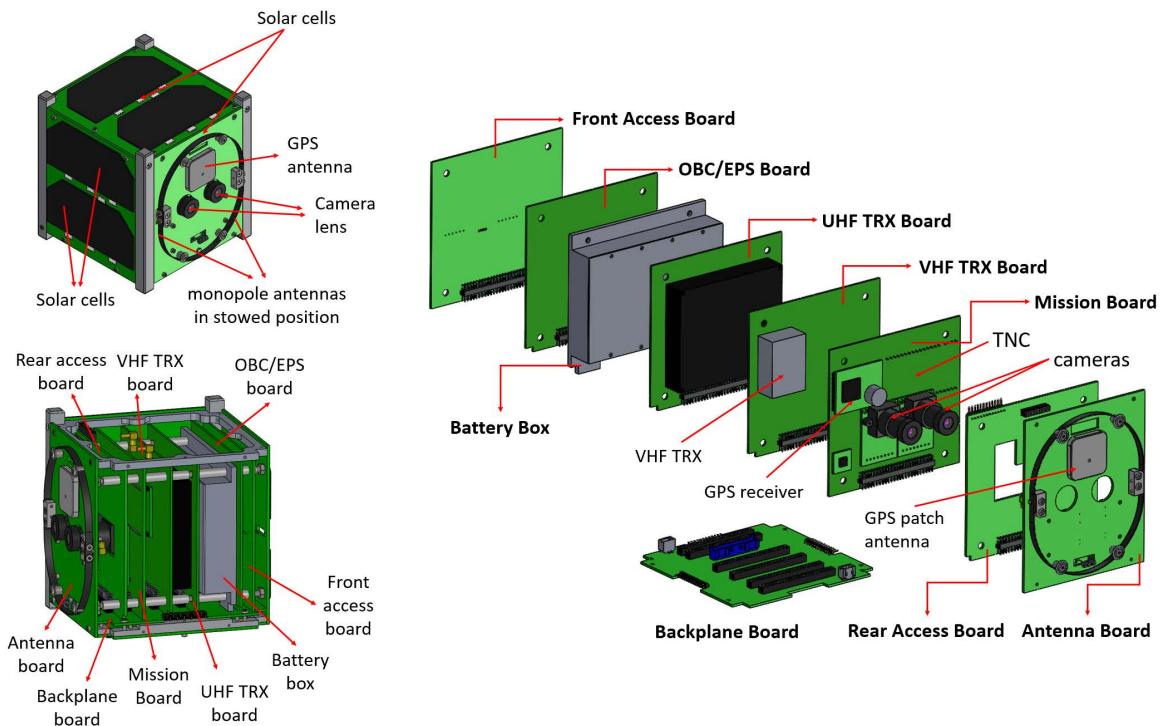


Figure 6 BIRDS-2 1U CubeSat drawings showing the internal and external boards

Table 1 shows the energy budget for operating the satellite in APRS-DP/S&F mission mode, assuming the payload is operating for 45 minutes in one orbit (~50% of one orbit duration) and RF transmission is active 25% of this time. Indeed, the energy budget is tight due to limited energy generation capacity from the solar cells for a 1U CubeSat and so a practical way to deal with this limitation is to activate the payload within a specified duration and timing (delay of turning on from receipt of command) through a ground station in one country before passing over the desired operation location in another region. The energy budget will be greatly improved by utilizing a 2U or 3U CubeSat platform for a full-time operational mission.

**Table 1 Energy budget of the satellite operating in APRS-DP/S&F mission mode**

Parts	Current (A)	Power (W)	Duration/Orbit (h)	Energy/Orbit (Wh)
Non-mission operation (OBC/EPS board, mission board, CW beacon TX, command RX)	0.0160	0.632	1.5	0.948
S&F payload (RX/standby)	0.080	0.316	0.5625 (75%)	0.178
S&F payload (TX)	0.390	1.541	0.1875 (25%)	0.289
Total for running APRS-DP/S&F payload on	-	-	-	1.415
Average energy generation/orbit (estimate)	-	-	-	~1.2 (conservative estimate)

### 2.3. Antenna Design and Deployment Mechanism Implemented on the BIRDS-2 CubeSat

The BIRDS-2 satellite consists of two deployable monopole antennas, as illustrated in Figure 7. One is a UHF antenna covering the UHF amateur band (430-440 MHz) and is used for uplink command reception, CW beacon transmission, and telemetry and mission data downlink. The other is a VHF antenna operating at 145.825 MHz and is used for both user uplink and downlink of the APRS-DP/S&F mission. These antennas are expected to have omnidirectional radiation patterns because the satellite only has a passive stabilization mechanism.

The antenna elements are made up of carbon tool steel (SK85(SK5) [23]) with thickness of 0.3 mm, width of 4 mm and quarter-wave lengths of 17.5 cm (UHF) and 50.1 cm (VHF). These elements are separately attached to a 3D printed plastic on the external side of +Y panel, secured to the plastic by tiny screws and carefully soldered to the inner conductors of MMCX connectors mounted on the panel's internal side. Then, short RF cables connect the antennas to respective transceivers. The whole structure is electrically connected to the satellite system ground. There are no matching networks in the BIRDS-2 design.

On the way to and during deployment from the ISS, antenna elements are stowed around mounting screws. Their ends are tied to a single fishing string (GOHSEN PE Hunter Lock No. 8 [24]) made of polyethylene (PE) material, which is securely tied to two lower mounting screws. The string passes through a coiled nichrome wire that will be heated up by a burner circuit 30 minutes after satellite deployment to burn the string and release the elements. The burner circuit draws high current from the battery through the EPS's unregulated voltage output. The nichrome wire resistance (i.e., number of turns) and burner circuit electrical settings were optimized for shorter burning time and higher deployment reliability. Further details on the antenna deployment mechanism and deployment test in cold temperatures are discussed in [25].

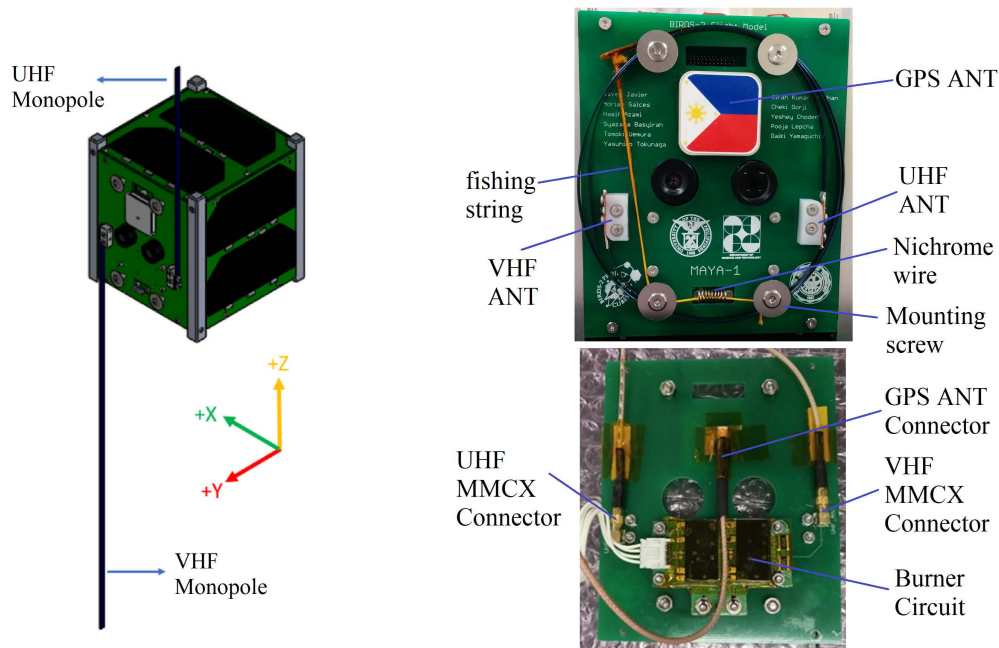


**Figure 7 Monopole antennas of the BIRDS-2 satellite in deployed condition (left); external side of antenna board showing the stowed elements (upper right); internal side showing the antenna connectors and burner circuit (lower right)**

#### 2.4. Design Improvements Implemented on the BIRDS-2S CubeSat's APRS-DP/S&F Mission Payload

When the APRS-DP/S&F payload of the BIRDS-2 CubeSats were automatically activated about a week after deployment from the ISS, it was found that downlink communication was working. We confirmed this at Kyutech ground station by being able to receive and decode the APRS beacon messages regularly transmitted by the payload (except for MAYA-1, which worked only a few times). Several reports from amateur operators around the globe submitted through an online submission platform of BIRDS-2, as well as received packets forwarded to Internet servers, supported this result. However, full digipeating and two-way communication with users failed due to uplink communication problem. The payload receiver could not properly receive and decode packets from users. The causes of failure uncovered from ground communication tests (details are discussed in Section 3) are:

- 1) satellite's VHF monopole antenna has poor matching and low gain due to improper RF grounding;
- 2) satellite's OBC/EPS board emits electromagnetic interference (EMI) that is captured by the antenna, thereby increasing the noise floor of payload receiver.

To address these problems, we explored two main changes targeted to be implemented on the BIRDS-2S satellite (an educational satellite project at the University of the Philippines-Diliman using a modified BIRDS-2 CubeSat design):

- 1) To minimize the dependence on grounding, a new antenna board was designed, consisting of a UHF dipole antenna for communication with GS and another VHF dipole antenna for the APRS-DP/S&F payload;
- 2) To reduce the EMI captured by the antenna, we tried shielding the satellite's OBC/EPS board with copper plate connected to ground. However, since this was determined to be ineffective, in future work, we plan to use an EMI absorber and shielding sheet commercially available.

The drawing and photos of the new antenna design for BIRDS-2S CubeSat are given in Figure 8, consisting of UHF and VHF dipole antenna elements that are purposefully oriented perpendicular to each other. Due to space constraint on the antenna board, the two respective elements of both dipole antennas could not be positioned directly beside each other. Thus, as shown in the antenna board layout drawing on Figure 9, they are fed by striplines routed on the second layer of the board through pads that are accessible on the top and bottom layers. A

jumper wire is attached to each element – one end of jumper wire is tightened by screw to the element while the other end is inserted into and soldered the pad on the back side of the board. (Note: the actual EM board in Figure 8 slightly differs from the PCB layout drawing on Figure 9, in which we adopted some modifications). Each stripline leads to the balanced input of either VHF or UHF balun. The unbalanced output of each balun is connected to a low-pass type L-matching network, which in turn is connected to a connector (SMA for UHF and MMCX for VHF) to which a cable going to respective transceiver will be connected. Due to limitation on available space, only the striplines of UHF dipole could be made equally long (which is more sensitive to phase offset than those of the VHF dipole).

In a previous test, to locate EMI sources in the satellite, we had probed different parts of the satellite and boards using a small loop antenna connected to a spectrum analyzer for EMI signal detection. The test setup is shown in Figure 10. This test demonstrated that the areas near some inductors of the switching power supplies (on the OBC/EPS board) were emitting significantly higher EMI levels compared to other parts of the board and the satellite. To reduce the EMI captured by the antenna, copper plates were attached to the front and back sides of the satellite's OBC/EPS board using Kapton tape, as shown in Figure 11. The copper plates were placed on a portion of the board in a way that would cover the inductors of switching power supplies and were electrically connected to the ground pins of the board by soldering jumper wires. To evaluate the effectiveness of the copper shield, a slightly different procedure was done using the satellite's own VHF antenna to directly measure the captured EMI, and this is described in Section 3.4. However, since this metallic shielding method was determined to be ineffective, in future work, we plan to explore alternative EMI mitigation methods such as commercially available products consisting of multiple layers of insulation, shielding and non-metallic absorption materials with overall thickness less than 1 mm.

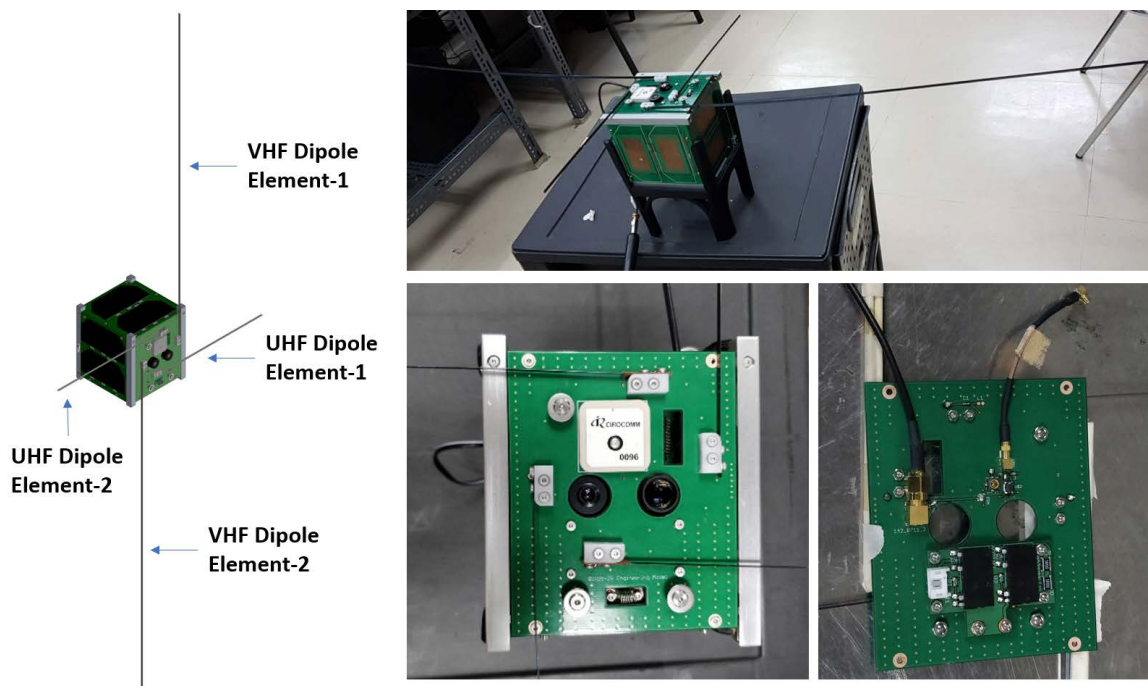


**Figure 8 New antenna design for BIRDS-2S CubeSat consisting of VHF and UHF dipole antennas: drawing (left), photos of actually implemented antennas for engineering model (right)**

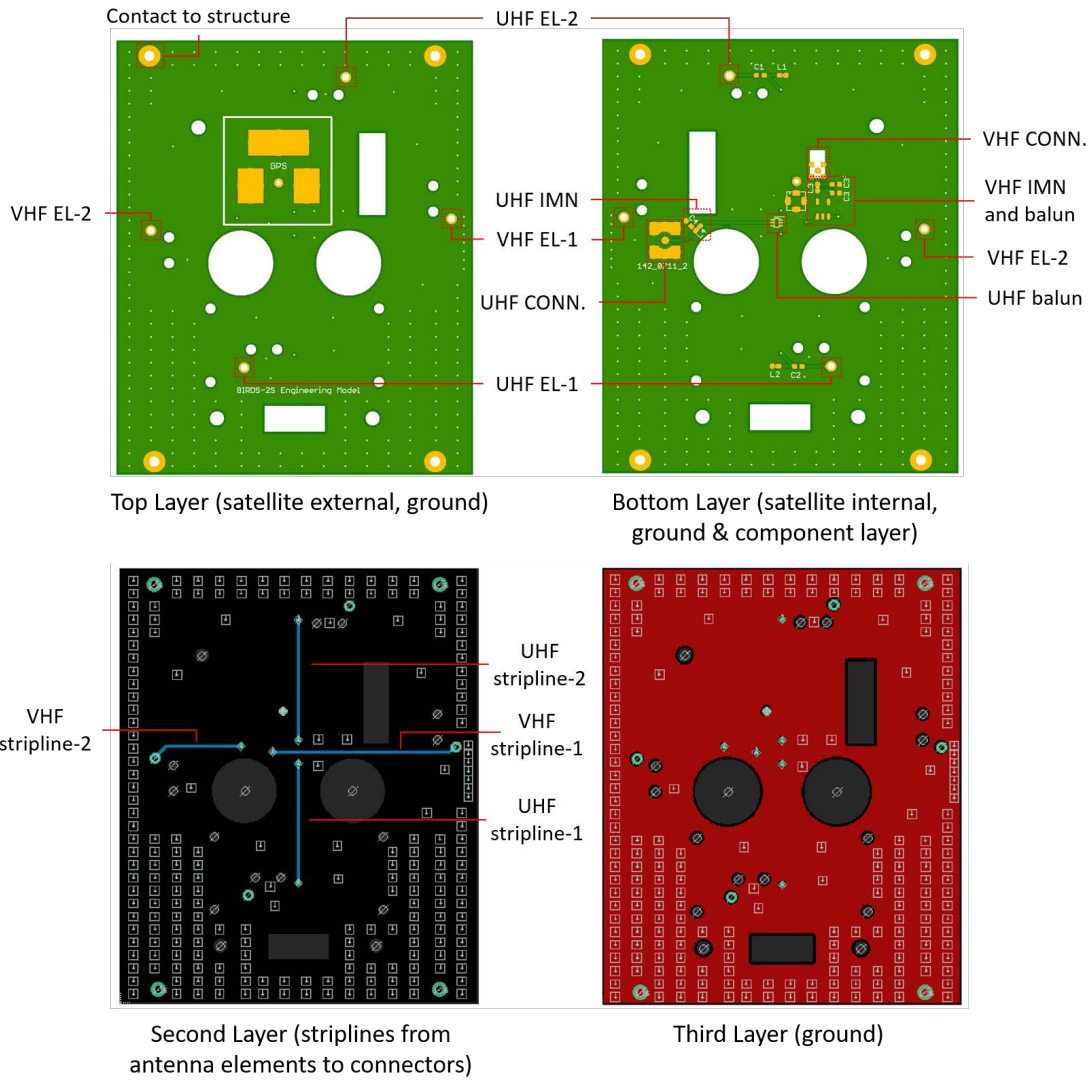


Figure 9 PCB layout of the four-layer antenna board for the BIRDS-2S CubeSat

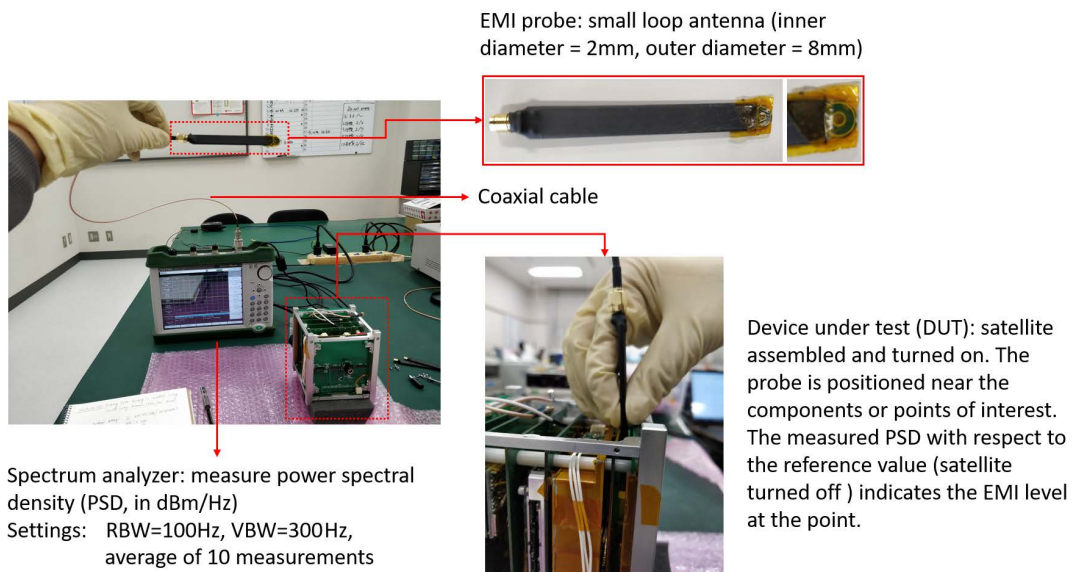
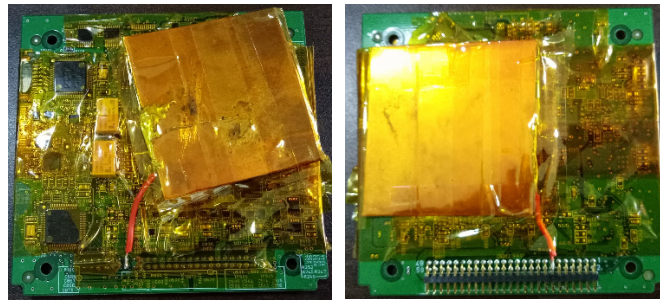


Figure 10 Test setup for locating the EMI-emitting sources in the satellite



**Figure 11** Photo of copper plate shielding on the OBC/EPS board of BIRDS-2S satellite: front side (left), back side (right)

**2.5. Design Improvements Implemented on the BIRDS-4 CubeSat’s APRS-DP/SF-WARD Mission Payload**

The design modifications implemented on BIRDS-4 APRS-DP/SF-WARD mission payload are like that of BIRDS-2S. There are two slight differences, though. First, instead of using the already assembled product for TT4, a kit version was used so that the components could be soldered directly on the mission board (instead of using an adaptor board, which was done in BIRDS-2 and BIRDS-2S). Second, the orientation between UHF and VHF dipole antenna elements are different: perpendicular in BIRDS-2S and non-perpendicular in BIRDS-4. A perpendicular arrangement is the most ideal, but it was not possible to implement in BIRDS-4 due to space constraint (other parts need to be put on the board such as perovskite solar cell). Also, the UHF antenna elements’ feed points are beside each other so they are connected to UHF balun without stripline. In addition to these two differences, the BIRDS-4 satellite has a modified OBC/EPS board design and it implemented an aluminum plate shielding. Figures 12 and 13 show BIRDS-4 CubeSat’s APRS-DP/SFWARD mission payload and antenna design, respectively.

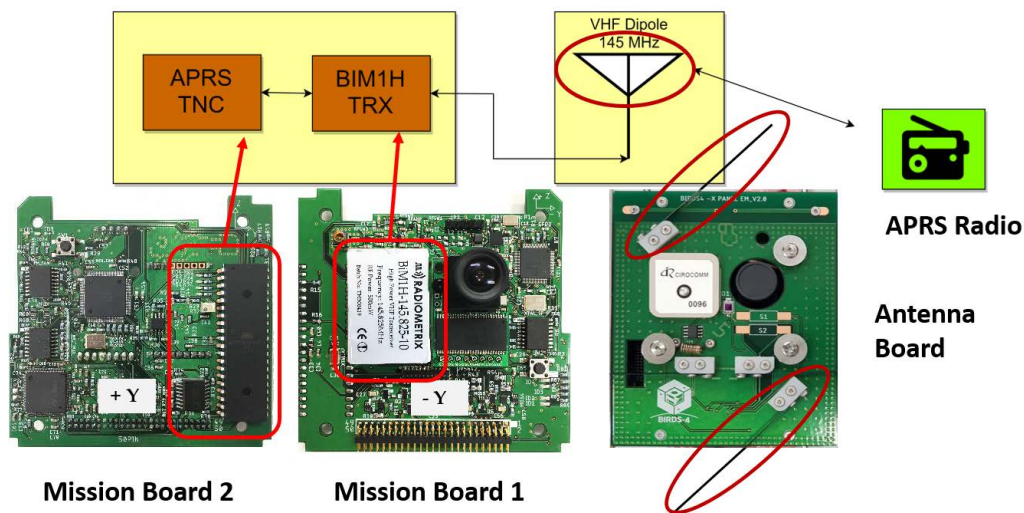


**Figure 12** BIRDS-4 CubeSat’s APRS-DP/SFWARD mission payload

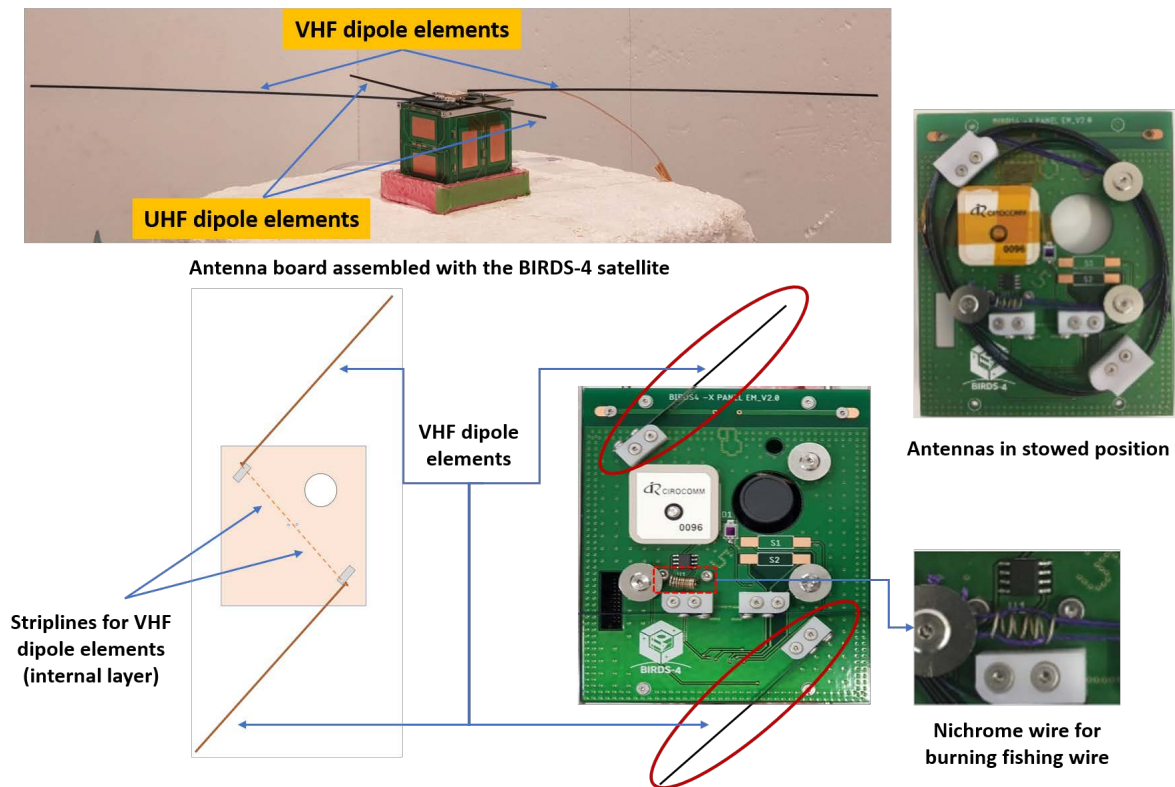


**Figure 13 BIRDS-4 CubeSat's VHF dipole antenna for the APRS-DP/SFWARD payload**

## 2.6. Satellite Integration and Space Environment Tests

During BIRDS-2 satellite development, the APRS-DP/S&F payload and other subsystems were assembled and integrated. Thermal vacuum and vibration tests were conducted on the fully integrated satellite to demonstrate the satellite would operate properly in space environment and would satisfy the launcher's safety requirements. To ensure reliability of antenna deployment mechanism, deployment tests were also performed in cold temperatures in a non-vacuum thermostatic chamber in different cold temperatures from  $-40^{\circ}\text{C}$  to  $-20^{\circ}\text{C}$  [25].

Thermal vacuum tests were done on both the engineering model and flight models to verify the functionality of the whole satellite and subsystems, including the APRS-DP/S&F payload, under vacuum condition and extreme cold and hot temperatures of space. This test would also confirm if the satellite and its parts can withstand the thermal stress under vacuum condition. This test was performed directly on the integrated satellite and unit level and subsystem level tests were skipped to save time and effort. In engineering model test, the satellite was subjected to  $-25^{\circ}\text{C}$  worst cold and  $+55^{\circ}\text{C}$  worst hot temperatures (control temperature is defined as the average of the six external panels' temperatures) for four thermal cycles. The payload was confirmed to be functional and survived the thermal cycling. In flight model test, the satellites were subjected to  $-25^{\circ}\text{C}$  worst cold and  $+65^{\circ}\text{C}$  worst hot temperatures for two thermal cycles.

Random vibration (20-2000 Hz, 6.53 Grms for QT, and 4.83 Grms for AT) and sine-burst vibration (18.1 G for QT) tests were performed on the engineering and flight models to demonstrate structural integrity of the satellites in rocket launch environment and to satisfy the launcher requirements. These were done as part of JAXA's acceptance process. The random vibration test profile used followed the combined envelopes for HTV and SpaceX launch vehicle profiles. The natural frequencies in all three axes were shown to be way higher than the minimum requirement of 100 Hz. During vibration test, the stowed antennas did not inadvertently deploy and there were neither dislocated nor removed parts. Thus, the satellites passed both qualification and acceptance vibration tests.

### 3. INVESTIGATION OF COMMUNICATION ISSUES THROUGH GROUND-BASED COMMUNICATION TESTS

Although we had performed a few communication tests during development, it was only in hindsight we realized that our test approach had limitations and that we committed serious mistakes in executing the test procedures. Some important aspects of communication verification test had been overlooked during development due to other pressing design issues, assembly, integration and test activities. Moreover, since the antenna design had undergone two iterations before being finalized, the team members working on the payload and antenna design did not have ample time to detect the antenna matching, grounding and EMI problems during integration. The failure to identify the real design issues was complicated by the fact that our existing measurement results at that time on antenna gain and reflection coefficient were incorrect, as well as the fact that we overlooked the satellite-radiated EMI. Also, between UHF and VHF communication subsystem verification tests, the team had to prioritize and dedicate more time for UHF communication subsystem because of its criticality for the whole satellite operation. It turned out, however, that both communication subsystems were facing similar problems.

In the subsequent portions of this paper, we discuss the results on the investigation conducted after the satellite had been delivered to the launch provider (and mostly after confirming failure of uplink communication after deployment from ISS). The presentation below reflects the improved and more systematic communication verification test procedure to address the limitations and mistakes from our previous communication tests during the satellite development.

#### 3.1. Determining the Actual Payload Receiver Sensitivity by Cabled Communication

Applying the SNR method [26], assuming a receiver bandwidth of 12 kHz and effective receiver noise temperature of 606 K, the estimated thermal noise power in the band is about -130 dBm. Then, for a threshold SNR of 21 dB (for AFSK/FM modulation at  $10^{-4}$  BER), the minimum receiver input power required is roughly -109 dBm. On the other hand, according to the product's datasheet, the receiver sensitivity is -120 dBm for 12 dB SINAD (signal-to-noise and distortion ratio, referring to analog signal quality). Thus, we can approximate that the 21 dB SINAD is 9 dB above -120 dBm or equal to -111 dBm, which is not far from the theoretical value (-109 dBm).

To determine the actual optimum sensitivities of uplink and downlink receivers, communication test between a Kenwood TH-D72 handheld radio (representing an APRS user or GST) and payload was performed in a cabled test condition. Figure 14 shows the test setup wherein the received RF power at the input of payload receiver was controlled by varying the attenuator value. The packet success rate was characterized for different values of receiver input power. The satellite (a flight spare) was placed inside an RF shield box to reduce the effect of possible leakage from the handheld radio transmitter to the payload receiver and vice-versa.

The packet downlink success rate (PDSR) and packet uplink success rate (PUSR) are plotted in Figure 15 for the case of matched frequencies and in Figure 16 for case of mismatched frequencies. In the figures,  $L$  is the total length in bytes of the test packet sent. To facilitate the discussion below, a threshold success rate of 80% is considered for sensitivity. For the case of matched frequencies, the optimum (cabled condition) uplink receiver sensitivity is within the range of -110 dBm to -114 dBm while the optimum downlink receiver sensitivity is within the range of -109 dBm to -111 dBm, depending on packet length. For the case of mismatched frequencies, a 5 kHz Doppler shift (only about 3 kHz is expected in practice) would result in a 4-7 dB worse receiver sensitivities – uplink receiver sensitivity of about -105 dBm and downlink receiver sensitivity of about -106 dBm, for a 100-byte packet length.

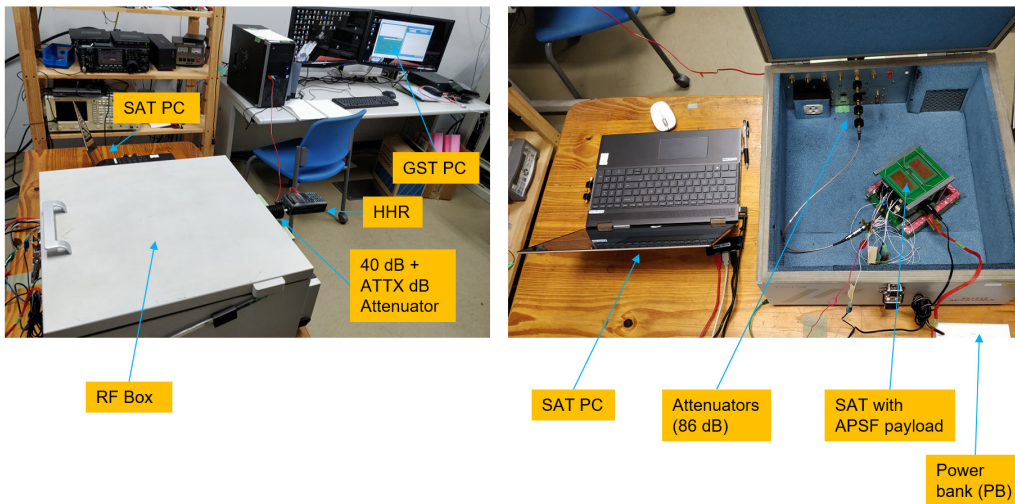
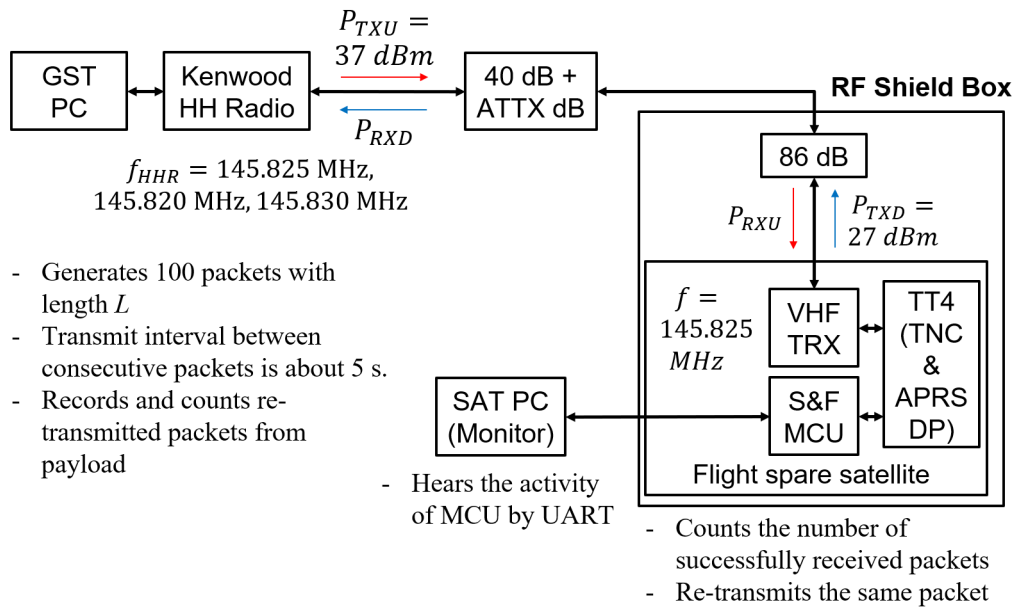


**Figure 14 Cabled communication test setup to determine the optimum uplink and downlink receiver sensitivities: (top) diagram, (bottom) photo of actual setup**

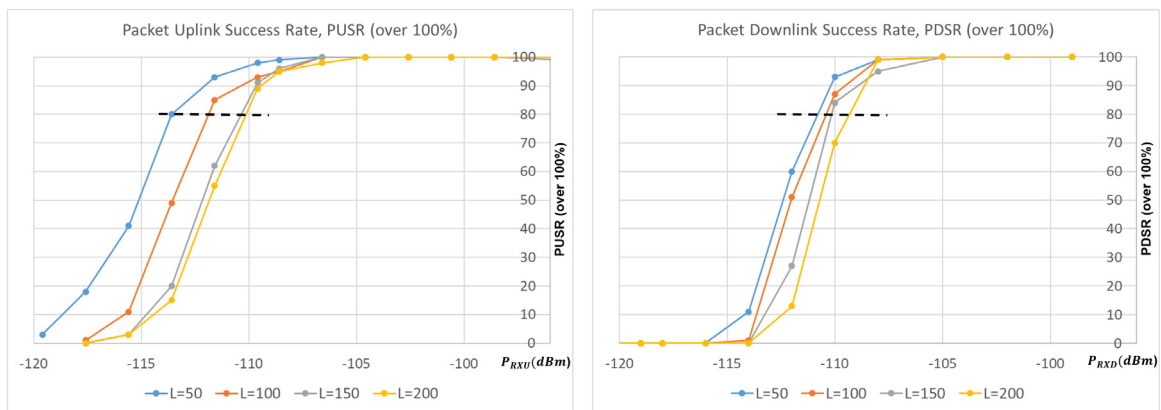


**Figure 15 Measured uplink and downlink receiver sensitivities in cabled test condition (matched TX and RX frequencies, representing no Doppler shift)**

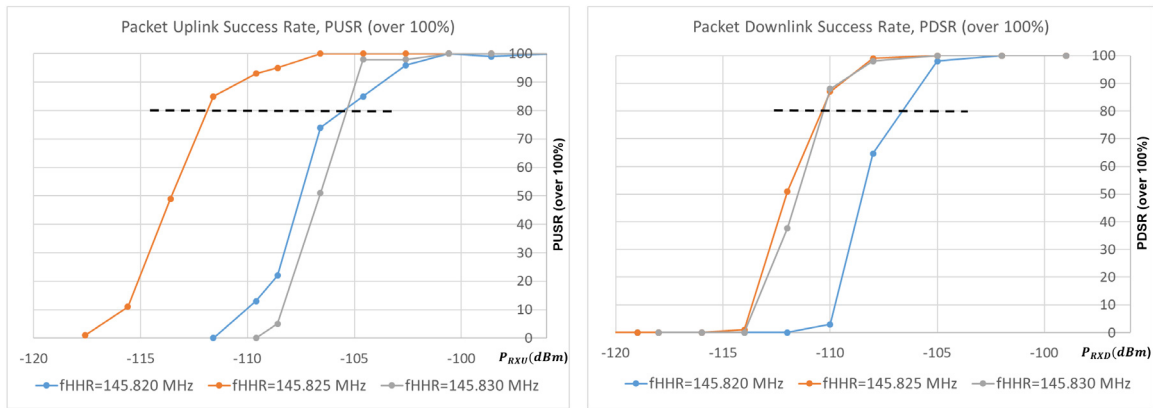


**Figure 16 Measured uplink and downlink receiver sensitivities in cabled test condition (mismatched TX and RX frequencies, representing 5 kHz Doppler shift,  $L=100$  bytes)**

### 3.2. Antenna Reflection Coefficient Measurement, Tuning and Radiation Pattern Test

The previous approach of measuring the antenna’s reflection coefficient ( $S_{11}$ ) using a VNA involved disconnecting the MMCX male connector of VHF cable from the MMCX female connector on the VHF transceiver (TRX) board (refer to Figure 4 bottom left) and connecting it to the VNA probe. This produced inaccurate measurement during BIRDS-2 antenna board testing because the VHF TRX board’s ground would be part of the satellite’s overall RF grounding in the real operation condition. To measure  $S_{11}$  more accurately, this time for the BIRDS-2S antenna board, we utilized a VHF TRX test board that is similar to the VHF TRX board but with another MMCX connector mounted at the point where the BIM1H transceiver’s RF pin would be soldered (note: VHF TRX not mounted on the test board). The test diagram is shown in Figure 17-2, wherein  $Z_m$  is the measured impedance just at the point representing the RF port of the transceiver. This enabled us to measure the  $S_{11}$  effectively at the transceiver’s RF port, with the VNA substituting for the transceiver in the test. Also, the VNA was calibrated at the end of the probe cable. A photo of the actual measurement setup for the case of the BIRDS-2S antenna board is shown in Figure 17-1.

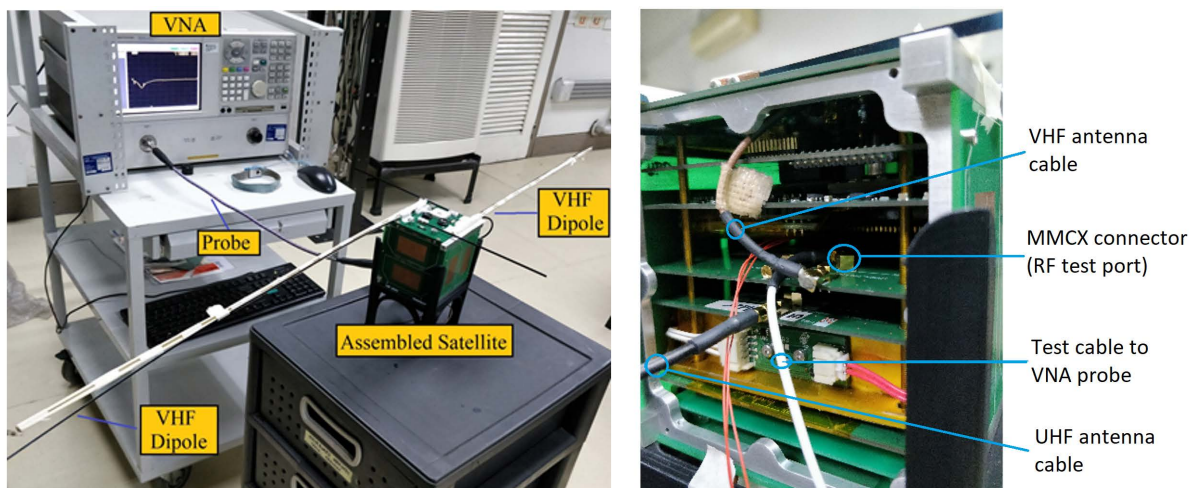


**Figure 17-1 Actual setup for antenna  $S_{11}$  measurement and tuning**

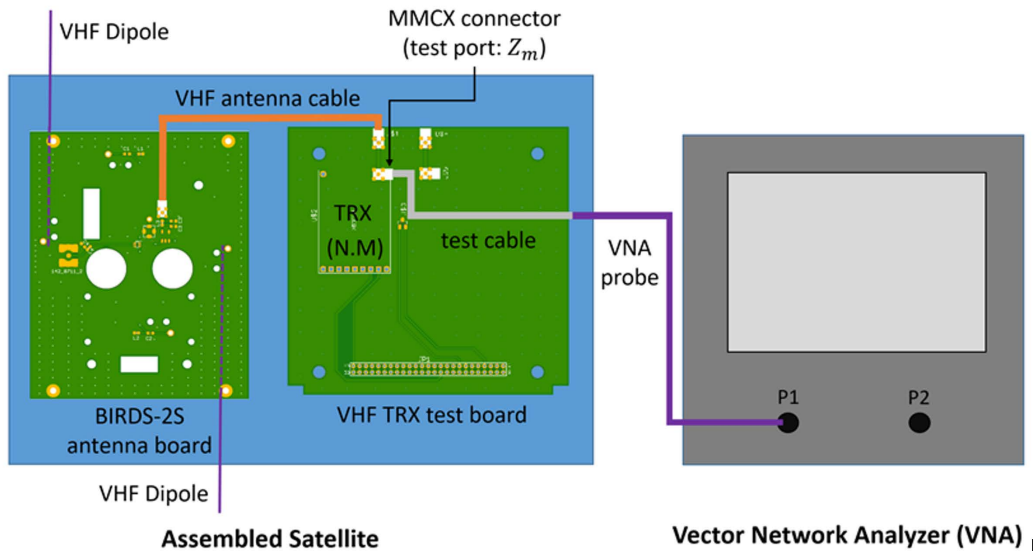


Figure 17-2 Setup diagram for antenna S11 measurement and tuning

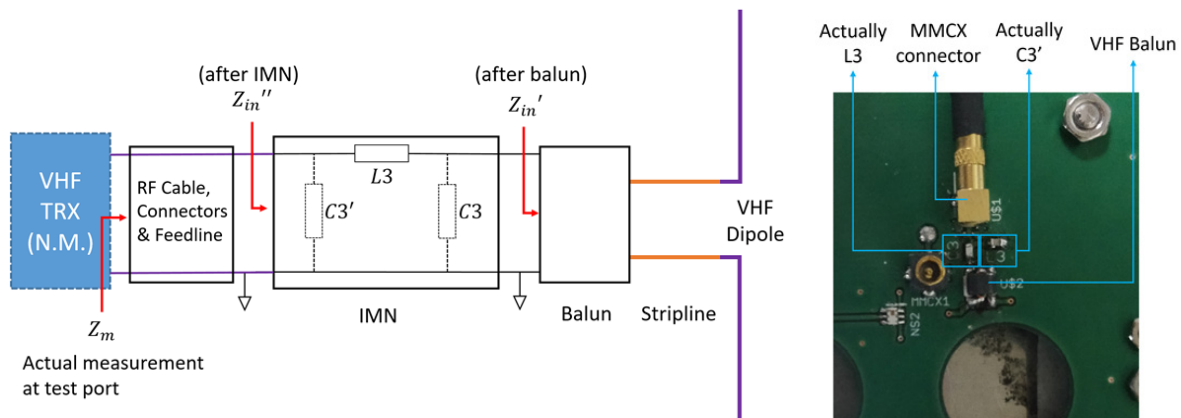
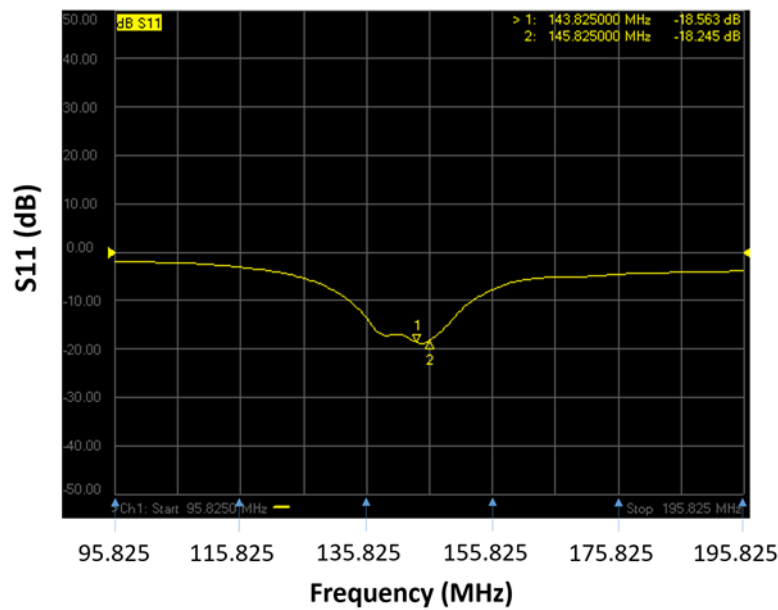


Figure 18 Circuit representation of the BIRDS-2S VHF dipole antenna parts and measurement setup (left) with a closer view of the actual antenna circuit implemented (right)

To better explain the antenna measurement, tuning and matching procedure, a circuit representation is provided in Figure 18 along with the actual circuit mounted on the antenna board. Tuning of the BIRDS-2S VHF antenna involved two steps. The first step entailed gradually cutting the antenna elements, starting from 65 cm on each element, until finding the length with maximum resistance  $R_m$  at 145.825 MHz. All impedance measurements are done only for  $Z_m$  because it was difficult to perform direct measurements of  $Z_{in}'$  (impedance after the balun) and  $Z_{in}''$  (impedance after the matching network). This was done without the impedance matching network (IMN) components connected (i.e., with  $L3$  pins shorted and  $C3/C3'$  pins left open). For every reduced length, the center frequency, reflection coefficient ( $S_{11}$ ), real and imaginary components of input impedance  $Z_m = R_m + jX_m$  at 145.825 MHz were recorded. As the length was reduced, the center frequency increased and  $R_m$  at 145.825 MHz increased, but only until a length 52 cm, where a maximum  $R_m = 61 \Omega$  was obtained. The  $Z_m$  at 145.825 MHz was equal to  $61 - j45 \Omega$  but the center frequency was lower than 145.825 MHz at this length. The second step required computing the values of IMN components and soldering them on the board. However, since we were left with a length of 50 cm (we cut 2 cm. more from 52 cm before realizing it was the best length) with a  $Z_m = 54.2 - j25.3 \Omega$  at 145.825 MHz, the values of IMN components were calculated for this length. The  $L3$  and  $C3$  obtained were 30.88 nH and 1.64 pF, respectively, but the actual components used were 33 nH and 1.8 pF, respectively.

The 1.8 pF capacitor was mistakenly mounted on  $C3'$  position. Nonetheless, since the calculated inductor and capacitor impedances at 145.825 MHz were  $j30.2 \Omega$  and  $-j606.3 \Omega$ , respectively, the transformed impedance was expected to be  $54.6 + j0.1 \Omega$ . Thus, the supposed effect was simply to almost eliminate the reactive part and leaving a real part that would result in a very good S11 ( $< -20$  dB). However, we actually obtained a  $Z_m = 67.7 - j17.0 \Omega$  and  $S11 = -13.9$  dB, which implies that the RF cable between antenna board and VHF TRX board and the feedline can change the impedance so that  $Z_{in}''$  and  $Z_m$  are actually different. Since our goal was to effectively match at the VHF TRX's RF port, we adjusted  $L3$  and  $C3'$  values and slightly reduced the antenna length to improve the S11. Finally, with 49.5 cm antenna length,  $L3 = 22$  nH and  $C3' = 1.5$  pF, we obtained  $Z_m = 57.9 - j12.2 \Omega$  and  $S11 = -18.2$  dB at 145.825 MHz, which are good enough. The resulting S11 plot is shown in Figure 19.



**Figure 19 Measured S11 of the BIRDS-2S VHF dipole antenna after tuning**

Radiation pattern and gain measurement of BIRDS-2 antenna board was conducted during BIRDS-2 development. However, the data were found later to be unreliable because of the following reasons: (1) the BIRDS-2 satellite, with mounted antenna board as the antenna-under-test (AUT), acted in receive mode, and in order to measure the received power by the antenna, the VHF antenna cable had to be disconnected from the VHF TRX board, hence this does not represent the realistic grounding condition (important aspect especially for monopole antenna); (2) the internal 10 dB attenuator of dipole antenna used as reference antenna was overlooked, so in the calculation of gain, the resulting values were 10 dB higher than the actual values; (3) there was not sufficient distance inside the anechoic chamber in Kyutech to achieve far-field condition for the VHF antenna case, so the measurements were probably still in the near field to far field transition region.

Antenna radiation pattern measurement was conducted again at the UPD's newly established full anechoic chamber facility (FAC) that utilizes a state-of-the-art near-field-to-far-field transformation technology (i.e., near-field measurements are transformed into far-field radiation pattern data, so far-field distance is not necessary). Also, as previously mentioned, we utilized a VHF TRX test board in this testing with another MMCX connector mounted at the point where the BIM1H transceiver's RF pin would be soldered. This allowed us to measure the effective gain that would be seen exactly at the transceiver's RF port. For direct comparison, radiation pattern measurement was performed on both BIRDS-2 antenna board and BIRDS-2S antenna board.

Figure 20 shows the actual radiation pattern measurement setup. On one side, the AUT (antenna under test, which refers to the commercial dipole antenna used as reference, or BIRDS-2 antenna or BIRDS-2S antenna) was attached to an L-bracket positioner and on the other side, the probe antenna (yagi) was fixed to a stand. The

probe antenna and the AUT were connected to RF cables leading to the two RF ports of the VNA outside chamber, which measured the total attenuation coefficient ( $S_{21}$ ) in terms of magnitude and phase. The system recorded the  $S_{21}$  values while rotating the positioner about the theta and phi axes with the probe antenna fixed in co-polarization (horizontal) position in the first scan. This step was repeated in the second scan with the probe antenna fixed in cross-polarization (vertical) position.

After scanning, the system applied a near-to-far-field transformation algorithm and provided the 3D far-field data in various elevation (EL) and azimuthal (AZ) planes defined with respect to the AUT. However, due to the blocking effect of absorbers on the positioner, the resulting far-field data was inaccurate in the region of the AUT facing toward the positioner. Therefore, five strategically selected initial AUT positions were tested (following the procedure just described here) and only the far-field data on the narrow region facing toward the probe (about  $90^\circ$ ) was extracted for each position. Then, the data extracted from the five positions were concatenated to obtain the radiation patterns on the antenna's E-plane and H-plane. A simple averaging filter was applied near the concatenation points to smoothen out the plots. Gain comparison method was used to estimate the gain in various directions, hence the radiation pattern in dB.

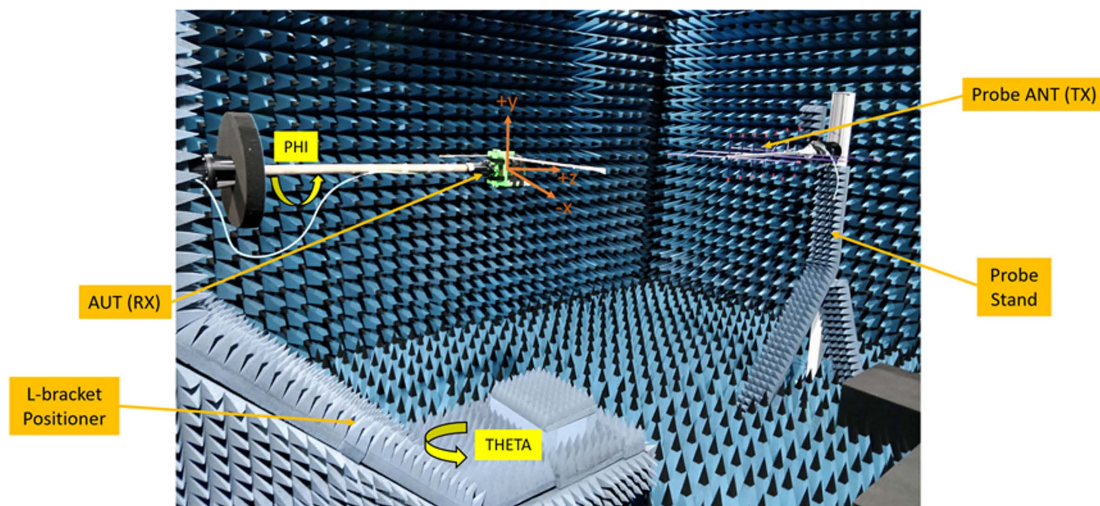


**Figure 20** Antenna radiation pattern measurement setup at UPD's full-anechoic chamber (FAC) facility

The resulting radiation patterns are presented in Figures 21 and 22 (the +z and other axes are the same as defined in Figure 20). Both BIRDS-2 and BIRDS-2S VHF antennas exhibit an omnidirectional pattern on the H-plane (perpendicular to the antenna element) and have nulls on the E-plane in the directions where the antenna elements are pointing. From the plots, the gain of the BIRDS-2 VHF monopole antenna is about -3 dB while the gain of the BIRDS-2S VHF dipole antenna is about 0.5 dB (note that the reference dipole antenna gain was assumed to be only 1.2 dB). These results demonstrate better gain performance of the new BIRDS-2S antenna design over the previous BIRDS-2 antenna design.

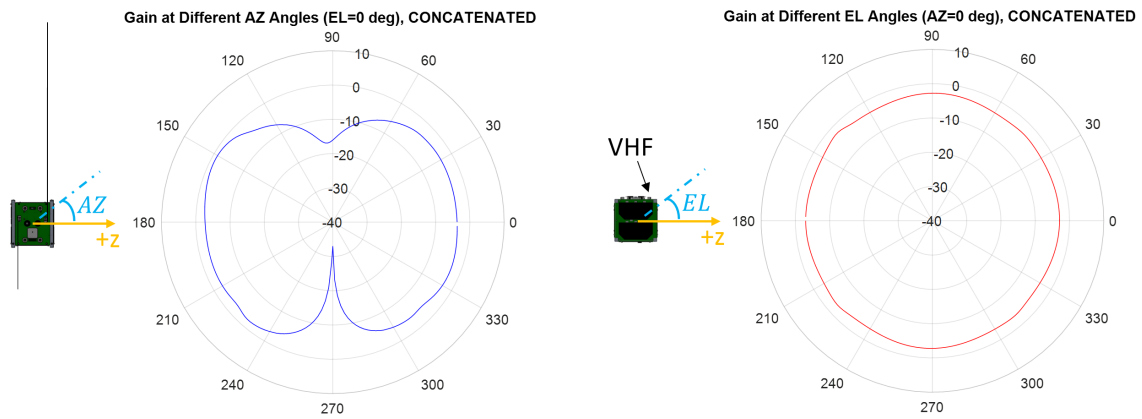


**Figure 21 Radiation pattern of BIRDS-2 VHF monopole antenna on E-plane (left) and H-plane (right). Gain is shown in dB**

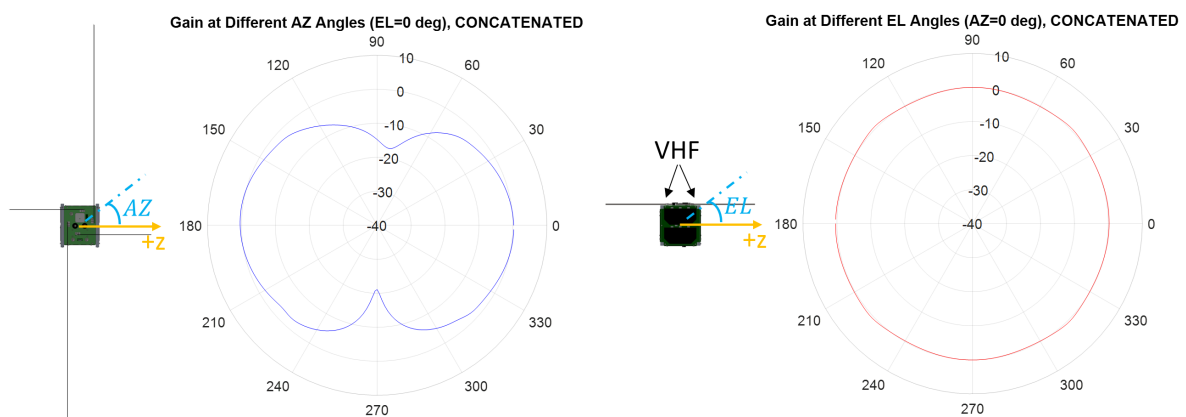


**Figure 22 Radiation pattern of BIRDS-2S VHF dipole antenna on E-plane (left) and H-plane (right). Gain is shown in dB**

### 3.3. Wireless Communication Tests Inside the Anechoic Chamber

To determine the actual payload receiver sensitivity in satellite-integrated and wireless condition, communication test between the satellite (with the payload and BIRDS-2S antenna board) and handheld radio (acting as an APRS user) was performed inside the FAC, with test setup shown in Figure 23. The distance between the satellite and dipole antenna (attached to attenuators and handheld radio outside the chamber) was confirmed to be about four meters. The received RF power at the payload receiver input was to be controlled by varying the attenuator value and then the uplink packet success rate would be recorded for each resulting receiver input power.

Before communication test, the setup was carefully checked and calibrated by measuring the transmitters' output powers, cable losses and free space path loss, considering the antenna gains obtained from previous tests. When the attenuator was initially set to 40 dB, the measured received power from the satellite antenna (using spectrum analyzer) was -30 dBm. Considering radio output power of 36 dBm, 1 dB cable loss, 1.2 dB transmit antenna gain, and 0.5 dB receive antenna gain, the free-space path loss was estimated to be about 26.7 dB (compared to theoretical value of 27.8 dB, assuming far-field free-space condition). Nonetheless, as part of the calibration procedure, the received power from the satellite antenna (equal to received power at the payload receiver input) was measured and recorded for each attenuator value. The measurement values confirmed that the receiver input power could be linearly (in dB) controlled by adjusting the attenuator value. To test the uplink communication, an APRS message (total packet length of about 50 bytes) was transmitted from the handheld radio.

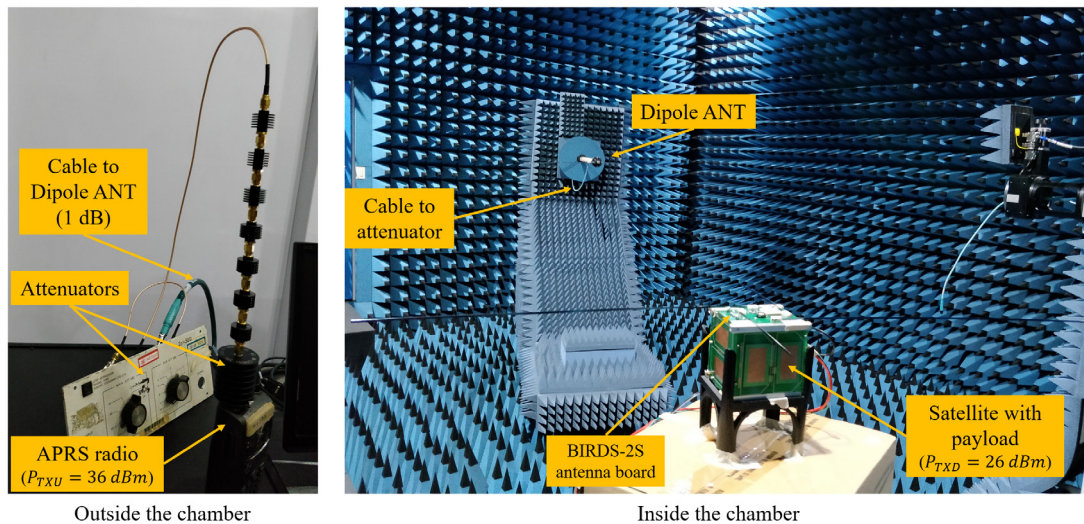


**Figure 23** Wireless communication test setup at UPD FAC for testing the payload receiver sensitivity using BIRDS-2S dipole antenna (APRS-DP communication test)

The experimental results for uplink success rate are tabulated in Table 2, which suggests an uplink receiver sensitivity of about  $-79$  dBm for a packet success rate of 70%. This wireless uplink receiver sensitivity result is 35 dB worse than the corresponding cabled test result of  $-114$  dBm (refer to Figure 15). This worse payload receiver sensitivity is due to the radiated EMI from the satellite that is captured by the dipole antenna and goes into the receiver, thereby increasing the effective “noise” floor. The increased noise floor also raises by the same amount the required threshold input RF power for successful demodulation. This is explained further in the next section.

Prior to the wireless communication test at the UPD FAC described above, a similar test procedure had been conducted at Kyutech’s full anechoic chamber involving BIRDS-2 satellite flight spare but using a commercial dipole antenna. Instead of using the handheld radio to transmit an APRS message, it was used to transmit a 100-byte S&F packet for 100 trials. The results are given in Table 3, indicating a payload receiver sensitivity of about  $-77$  dBm (for a 65% success rate) when using a commercial dipole antenna. This is comparable to the payload receiver sensitivity of  $-79$  dBm (for a 50-byte APRS packet, 7/10 success rate) when using the BIRDS-2S dipole antenna in the UPD FAC communication test. This suggests roughly equal communication performance of the BIRDS-2S dipole antenna when benchmarked against the commercial dipole antenna.

**Table 2** Experimental values for APRS packet success rate at different payload receiver input power using BIRDS-2S dipole antenna

Attenuator Value (dB)	Expected Receiver Power (dBm)	Measured Receiver Power (dBm)	Uplink Packet Success Rate
40	-30	-30	~10/10 (full success)
65	-55	-54	~10/10 (full success)
90	-80	-79	7/10
93	-83	-82	2/10
96	-86	-86	fail
99	-89	-88	-
102	-92	-92	-
105	-95	-94	-
108	-98	-97	-

**Table 3 Experimental values for S&F packet success rate at different payload receiver input power using a commercial dipole antenna**

Attenuator Value (dB)	Received Power (dBm)	Uplink Packet Success Rate (out of 100 trials)
40	-32	-
70	-62	-
75	-67	100%
81	-73	98%
83	-75	96%
85	-77	65%
87	-79	39%
89	-81	12%

### 3.4. Payload Receiver Noise Level Measurements

The 35 dB worse uplink receiver sensitivity in wireless (antenna connected to satellite) test condition from its optimum value in cabled test condition can be accounted on the increased noise level in the payload receiver due to the radiated EMI from the satellite that is captured by the dipole antenna. To confirm this, we measured the received signal strength indicator (RSSI) voltage of the VHF TRX (BIM1H transceiver) in two conditions (RSSI voltage is an indicator of the receiver RF power estimate that is provided on an analog pin of BIM1H transceiver). In the first condition, the BIRDS-2S dipole antenna was disconnected from the transceiver RF port (open). Then, in the second condition, the dipole antenna was connected to the transceiver RF port. The test was conducted with the assembled BIRDS-2S satellite inside the anechoic chamber, as shown in Figure 24. The receiver input RF power level or the noise level in this test, could be estimated from the plot of the RSSI voltage vs RF level that is provided on BIM1H datasheet (which we had confirmed to be a good indicator of RF power level in a previous calibration test).

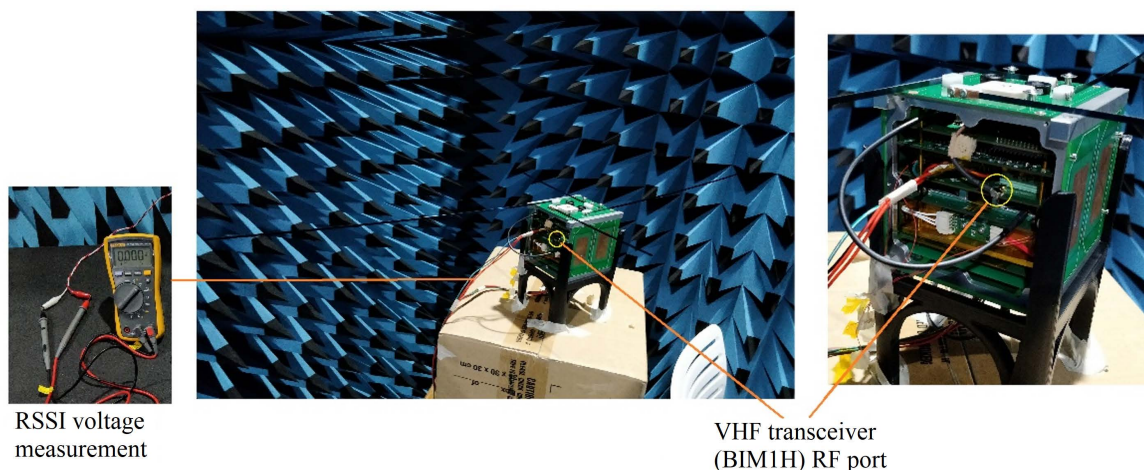


**Figure 24 Test setup for detecting noise level increase in the payload receiver due to satellite-radiated EMI captured by the antenna. This was done inside UPD FAC.**

The first condition represents the case wherein the satellite-radiated EMI is present but does not go into the receiver, hence the RSSI voltage indicates only the thermal noise level in the receiver in this condition. The second condition represents the case wherein the satellite-radiated EMI captured by the dipole antenna is

transferred to the payload receiver, hence the RSSI voltage indicates the total noise level in the receiver (thermal noise and radiated EMI) in this condition. For comparison, the same procedure was performed with the BIRDS-2 monopole antenna. Finally, we put the copper plate shielding previously described to test its effectiveness and repeated the whole procedure.

The measurement results for the case before putting the copper plate shielding are provided in Table 4. With either antenna board integrated to the satellite but the VHF antenna disconnected from the VHF TRX port, an RSSI voltage of about 0.4 V was recorded, corresponding to an estimated noise level of -135 dBm. This value happens to be the minimum RF level detectable by the RSSI voltage (in the RSSI voltage vs RF level plot) and is not far from the theoretically estimated thermal noise power of about -130 dBm. Thus, it is very likely that thermal noise is the dominant noise present in the payload receiver when no antenna is connected. When either VHF antenna is connected, however, one can clearly see a large increase in RSSI voltage and estimated RF level: 39 dB increase for the case of BIRDS-2S dipole antenna and 53 dB increase for the case of BIRDS-2 monopole antenna. Note that the 39 dB increase in receiver noise level for the BIRDS-2S dipole antenna case may account for the 35 dB worsening of uplink receiver sensitivity observed during the wireless communication test. The measurements for the case after putting the copper plate shielding are given in Table 5 and demonstrates that this shielding approach is not effective in attenuating the satellite-radiated EMI (in the case of the BIRDS-2S).

**Table 4 Receiver noise level from RSSI voltage without copper plate shielding**

Condition	BIRDS-2 VHF Monopole Antenna (BIRDS-2 antenna board integrated)		BIRDS-2S VHF Dipole Antenna (BIRDS-2S antenna board integrated)	
	RSSI Voltage (V)	Estimated RX Power (dBm)	RSSI Voltage (V)	Estimated RX Power (dBm)
	Satellite and payload on, BIM1H RF port open	0.40	-135	0.39
Satellite and payload on, BIM1H RF port connected to antenna	1.55	-82	1.22	-96

**Table 5 Receiver noise level from RSSI voltage with copper plate shielding**

Condition	BIRDS-2 VHF Monopole Antenna (BIRDS-2 antenna board integrated)		BIRDS-2S VHF Dipole Antenna (BIRDS-2S antenna board integrated)	
	RSSI Voltage (V)	Estimated RX Power (dBm)	RSSI Voltage (V)	Estimated RX Power (dBm)
	Satellite and payload on, BIM1H RF port open	0.37	-135	0.38
Satellite and payload on, BIM1H RF port connected to antenna	1.43	-87	1.22	-96

### 3.5. Long Range Communication Test (LRT)

A long-range communication test (LRT) was conducted between a fully integrated BIRDS-4 EM satellite (with APRS-DP/S&F payload) and an APRS user radio (Kenwood TH-D72). The same test was repeated with a

fully integrated BIRDS-4 FM satellite. A similar test will be conducted on the BIRDS-2S satellite after a better shielding approach is implemented. The objective of the LRT is to confirm the link budget in a test setup emulating ground-satellite distance. It is similar to that of the wireless test inside the FAC but since it is done in an outdoor environment, it has the following main differences: (a) the large distance between satellite and APRS user radio antennas ensures that the two sides communicate in very far-field condition (much more than what could be achieved inside the FAC); (b) the channel between the two sides is not free-space so there are reflections and other propagation effects, but the lumped attenuation due to these could be determined during calibration procedure; (c) external devices in the vicinity (e.g., noise and interference sources) could impact the test, hence, the satellite is subjected to more noisy environment in this condition than inside an FAC or in space.

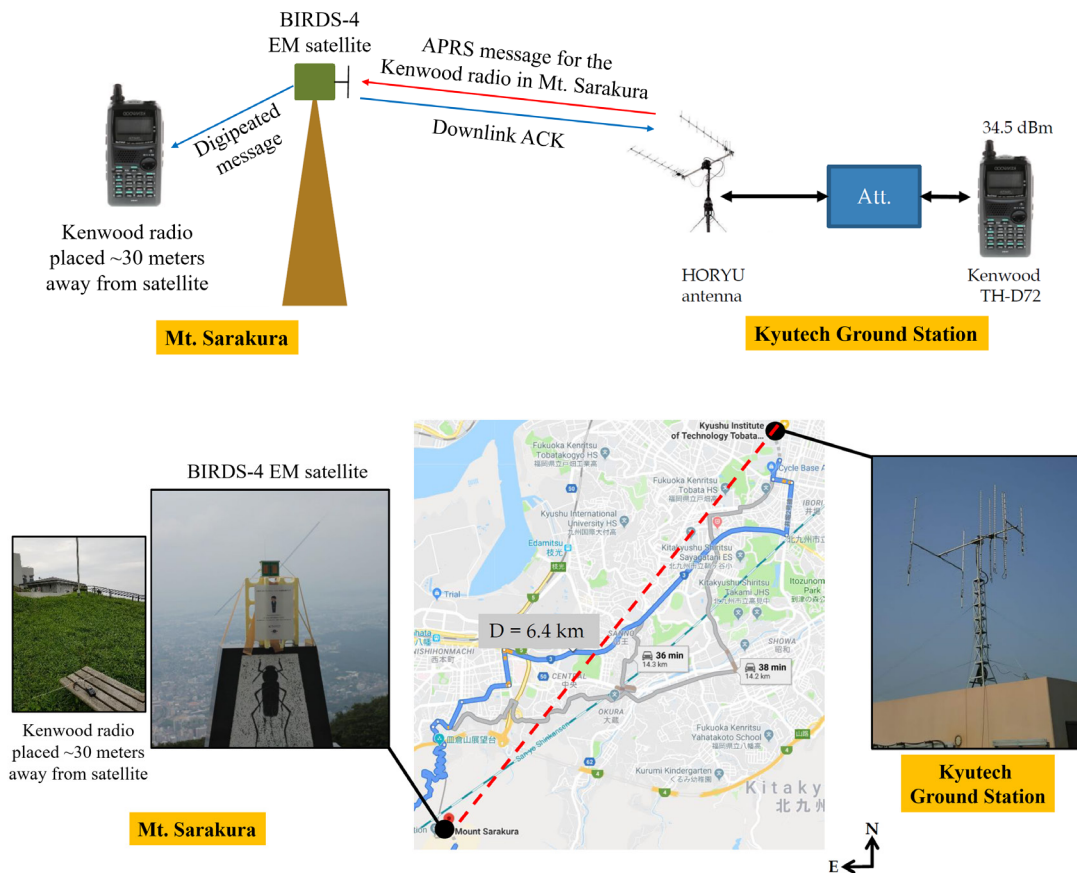


**Figure 25 BIRDS-4 long-range communication test setup involving the BIRDS-4 EM satellite**

The BIRDS-4 LRT setup is shown in Figure 25. The satellite and an APRS radio were placed in Mt. Sarakura that is located 6.4 km away from Kyutech. At Kyutech, another APRS radio with transmit power of 34.5 dBm was connected to the ground station’s yagi antenna with an attenuator in between. The attenuator value was gradually increased, and communication was tested for each attenuator value. In the LRT involving BIRDS-4 EM satellite, uplink success was achieved up to 130 dB effective attenuation (channel, antenna, cable, attenuator), implying a payload receiver sensitivity of about -95 dBm. On the other hand, a very close value of -96 dBm was obtained in the LRT involving BIRDS-4 FM satellite. This BIRDS-4 payload receiver sensitivity is 16-17 dB better than the BIRDS-2S payload receiver sensitivity (-79 dBm) obtained in wireless communication test inside the FAC. The better receiver sensitivity obtained on BIRDS-4 payload receiver suggests lower receiver noise is induced by the EMI from the BIRDS-4 satellite, compared to the case of BIRDS-2S satellite. Although one possible reason is the different OBC/EPS board components arrangement and layout, combined with aluminum plate shielding attached on the OBC/EPS board, further investigation and experiments are needed

confirm this. At this point, the exact cause of improvement of BIRDS-4 payload receiver sensitivity is not certainly determined.

### 3.6. Communication Link Budget Analysis

The link margin in uplink and downlink paths were calculated based on the parameters summarized in Table 6 for two cases of GS (GST or APRS user) antenna: (a) 16 dBi directive (cross-Yagi) antenna with pointing, and (b) 5.6 dBi omnidirectional antenna (“Eggbeater” antenna [27]) with fixed position and 120° beamwidth. Both GS antennas are circularly polarized. The main lobe of the omnidirectional antenna is assumed to be pointing upward (90° elevation) and so the GS antenna pointing error depends on satellite elevation. For the link margin calculations, we considered the experimental uplink receiver sensitivity of -95 dBm (obtained from BIRDS-4 LRT) and downlink receiver sensitivity of -105 dBm (obtained from actual RF power measurements on regular beacon signals received from BIRDS-2 satellites).

**Table 6 Parameters used in link margin calculation**

Parameter	Value
Orbit altitude	400 km
Center frequency	145.825 MHz
GS transmit power (uplink)	Kenwood TH-D72 handheld radio: 5 W (37 dBm)
Satellite transmit power (downlink)	0.5 W (27 dBm)
GS antenna gain	directive: 16 dB (yagi antenna), omnidirectional: 5.6 dB (Eggbeater antenna)
Cable loss at GS side	2 dB
GS antenna pointing error, $APE_{GS}$	directive antenna (with pointing): 5°, omnidirectional (fixed): $APE_{SC} = 90^\circ - \text{elevation}$
GS antenna pointing error loss ( $APE_{LGS}$ )	directive antenna: 1 dB, omnidirectional antenna: $APE_{LGS} = -10 \log(\cos(APE_{GS}))$
Polarization loss	3 dB
Atmospheric and ionospheric losses	1.8 dB
Satellite antenna pointing error loss ( $APE_{LSC}$ )	3 dB
Satellite antenna gain & cable loss	0.5 dB
Free-space path loss (FSPL)	127.8 dB (at EL=90°) to 143.0 dB (at EL=0°)
Received power (dBm)	<u>Uplink</u> Omnidirectional: -118.2 (at EL=5°) to -94.5 (at EL=90°) Directive: -98.2 (at EL=5°) to -85.1 (at EL=90°)
	<u>Downlink</u> Omnidirectional: -128.0 (at EL=5°) to -104.5 (at EL=90°) Directive: -108.2 (at EL=5°) to -95.1 (at EL=90°)
Receiver sensitivity (dBm)	Uplink: -95 (payload receiver), Downlink: -105 (GS receiver)

The plots of the uplink and downlink margins vs elevation angle are given in Figure 26, for the two GS antenna cases. Although the downlink transmit power is 10 dB lower than the uplink transmit power, the required minimum receiver power is 10 dB lower in downlink than in uplink. This is the reason why overall, the uplink margin and downlink margin plots for a given GS antenna appear the same. These plots indicate the required minimum elevation angles of 15° and 75° for the directive and omnidirectional GS antenna cases, respectively. Therefore, only amateur stations with 16 dB or higher gain circularly antennas can be expected to effectively communicate with the payload. The uplink margin may be improved once the satellite noise problem is more effectively addressed but the limited downlink transmit power will remain a bottleneck for the downlink margin.

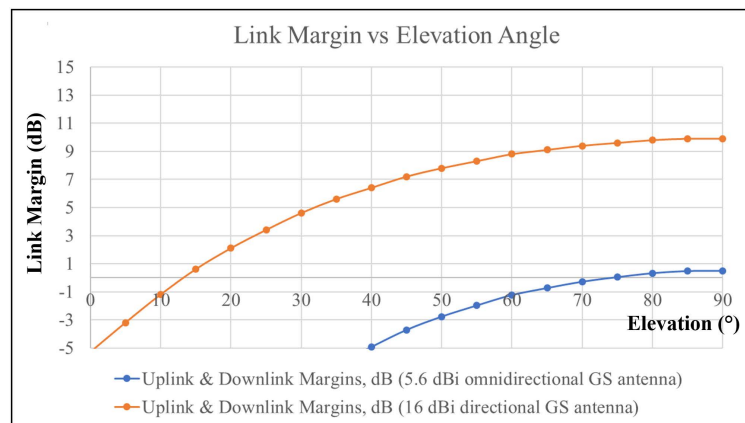


Figure 26 Uplink and downlink margins for the two GS antenna cases

#### 4. LESSONS LEARNED AND RECOMMENDATIONS FROM INVESTIGATION ON COMMUNICATION ISSUES

From the investigation we conducted and our experiences in BIRDS-2 Project and succeeding BIRDS projects in the matter of communication design for our CubeSat-onboard amateur radio payload (i.e., the APRS-DP/S&F payload), we summarize the following lessons learned and recommendations:

- 1) Since the antenna characteristics (tuning, grounding, performance) and EMI/EMC aspects (coupling, grounding, shielding, etc.) are intricately related to one another, as well as to the whole satellite structural and electrical power design considerations, these aspects must be altogether examined and verified through practicable methods during the preliminary design phase of satellite development. As the parts are closely positioned inside a CubeSat, it is crucial to consider the potential EMI/EMC issues in the design of the whole satellite. For the case of BIRDS-2 Project, the design issues related to these aspects were overlooked and lately diagnosed (even beyond the development time), so we could not address them proactively. On hindsight, the BIRDS-2 CubeSat bus design was adopted from a previous design without careful consideration of these issues.
- 2) Optimum receiver sensitivity performance must be verified in transceiver unit level, first in a cabled condition and then in a wireless (antenna-connected) condition in the early phase of development, that is, before integrating with other satellite subsystems.
- 3) Also, during the early phase of development, antenna reflection coefficient (and tuning) and radiation pattern tests must be done with pre-existing or mock-up satellite structure and boards. Similarly, subsystem boards, such as EPS board, must be tested to check if they might contribute significant EMI levels, whether conducted or radiated type. In the case of BIRDS-2, we found out later by using small loop antenna that the switching inductors on the OBC/EPS board emit significantly higher EMI levels compared to other parts of the boards and the satellite.

- 4) Then, antenna and EMI/EMC designs must be verified as soon as possible through antenna performance and EMI/noise measurement tests with the fully integrated satellite (for example, during activities leading to CDR). Aside from design verification, this is also necessary to diagnose potential design problems and mechanisms previously unconsidered and to find ways to mitigate these issues (e.g., adding EMI absorbers or shielding, filtering, modify signal routing and grounding, etc.).
- 5) Antenna tuning, S11 and radiation pattern measurements should be done as close as possible to the real operational condition, that is, how the antenna will be connected to a cable, transceiver board, grounding, satellite, etc.
- 6) In terms of antenna design, if the space constraints allow, dipole antenna is recommended over monopole antenna as the former's tuning and performance characteristics are less vulnerable to grounding issues. From our own experience in BIRDS-2 antenna development, we found that a monopole antenna is highly sensitive to size and configuration of grounding, which is especially difficult to optimize in a 1U CubeSat due to limited space. Also, from our own measurement data, the antenna's susceptibility to satellite-radiated EMI (or the amount of EMI coupled to the antenna) seems to be intricately related the quality of grounding of a monopole antenna. While we could have modified the BIRDS-2 monopole antenna design to mitigate the grounding and EMI vulnerability issues, we think that a dipole antenna design is the more conservative and less risky design choice to begin with because in principle, its performance is independent of a ground plane, unlike monopole antenna. Still, even if one uses a dipole antenna, one must still consider (5) because the matching network on the antenna board is connected after the unbalanced side of the balun, so the actual impedance itself and the measurement may be affected by the grounding and the cable from the antenna board to the VHF TRX board.
- 7) Wireless communication test inside a full-anechoic chamber and long-range communication test – between the fully integrated satellite and a ground station or user radio – must be done as final confirmation of end-to-end performance and the link budget analysis.

## 5. CONCLUSION

This work developed a CubeSat-onboard amateur radio payload that supports both APRS Digipeater and S&F communication for remote data collection. The aim was to leverage on CubeSat platform's simple architecture, short development time and low cost for these applications, while dealing with tight constraints on space, power and link budget. The APRS-DP/S&F payload was designed to operate at the VHF amateur frequency (145.825 MHz) to make it easily available for use by the global amateur radio community. The present paper tackled the design, development and testing of the APRS-DP/S&F payload onboard the BIRDS-2 CubeSat constellation, as well as the findings from the investigation on uplink communication failure. The payload can be accommodated on a 1U CubeSat platform for limited operation time or on a 2U/3U CubeSat platform for full-time operation. It consists of very low-cost COTS components selected for having small form factor, low power consumption, ease of interfacing and little programming work required for the development. Overall, the payload occupies about ¼ of the space on the mission board (which also hosts other subsystems and mission payloads), except for the VHF transceiver placed on a separate board and the dipole antenna mounted on an external board. The payload itself consumes only about 0.29 W while in receive or standby mode and 1.4 W during active RF signal transmission. It underwent various functionality, communication and space environment verification tests during development.

After the satellites' deployment into 400km 51° inclination orbit, it was confirmed that receiving the beacon messages regularly transmitted by the payload was working, but full two-way communication failed due to uplink communication problem. Our post-development investigation through ground-based communication tests found that the uplink failure was caused by two design problems that were overlooked during development, namely, the poor antenna performance and increased payload receiver noise floor due to satellite-radiated EMI coupled to the antenna. The latter problem increased the required receiver input RF power by over 50 dB in the original BIRDS-2 design, thus degrading the receiver sensitivity by a tremendous amount.

Our experience and investigation emphasize four important recommendations. Firstly, since the antenna

characteristics and EMI/EMC aspects are intricately related to one another in a 1U CubeSat with compactly positioned parts, these aspects and altogether with the satellite's structural and EPS designs, must be carefully examined during the preliminary design phase of satellite development. Secondly, the optimum cabled condition receiver sensitivity and the antenna (with pre-existing or mock-up satellite structure and boards) performance must each be tested in early phase of development. In terms of antenna design, if the space constraints allow, dipole antenna is recommended over monopole antenna as the former's characteristics are less dependent to grounding. Similarly, subsystem boards, such as EPS board, must be checked if they might contribute significant EMI levels, whether conducted or radiated form. Thirdly, antenna performance, EMI and receiver noise measurement tests must be performed with the fully integrated satellite as soon as possible. Mitigation approaches such as adding EMI absorbers or shielding may be considered upon diagnosis of previously unconsidered problems. Lastly, wireless communication tests inside a full-anechoic chamber and in outdoor very long-distance condition must be done as final confirmation of end-to-end performance and the link budget analysis. For further work, we also recommend to conduct a more comprehensive and systematic study that will examine the EMI/EMC related design issues on CubeSat platforms and provide guidelines to proactively address or mitigate issues that usually arise in very compact CubeSat platforms.

### ACKNOWLEDGEMENT

This work was supported by the JSPS Core-to-Core Program, B. Asia-Africa Science Platforms. A part of this research was supported by "Coordination Funds for Promoting AeroSpace Utilization", the Ministry of Education, Culture, Sports, Science and Technology (MEXT), JAPAN. The authors would like to thank their colleagues and partners in the BIRDS network for the collaborative works on BIRDS CubeSat projects and ground station network. They thank the members of BIRDS ground station network and the amateur radio community for their assistance in satellite operation. Kyutech has cooperated with the Philippine Department of Science and Technology (DOST) and UPD in the implementation of BIRDS-2, BIRDS-2S and BIRDS-4 CubeSat projects, which have been instrumental platforms for implementing the research described in this paper.

The first author appreciates the UPD Electrical and Electronics Engineering Institute (EEEI), as well as the faculty, staff and members of the STEP-UP Project, for allowing him to use the full-anechoic chamber facility, support during communication testing and sharing their insights on antenna design improvement. The first and second authors gratefully acknowledge the DOST-PCIEERD, DOST-SEI and UPD for the scholarship support they have received during their doctoral studies through the PHL-MICROSAT/STAMINA4Space Program.

### REFERENCES

- [1] R. Diersing, G. Jones, *Low Earth-Orbit Store-And-Forward Satellites in the Amateur Radio Service*, IEEE AES Systems Magazine, **8**(1), 21-30, 1993.
- [2] M.N. Allery, H.E. Price, J.W. Ward, R.A. Da Silva Curiel, *Low Earth orbit microsattellites for data communications using small terminals*, Proceedings of the 10th International Conference on Digital Satellite Communications, October, 1995.
- [3] PCSAT-1, Amateur Radio Satellite NO-44, <http://aprs.org/pcsat.html>
- [4] LAPAN-A2 microsattelite of Indonesia, <https://directory.eoportal.org/web/eoportal/satellite-missions/l/lapan-a2>
- [5] Diwata-2, <https://phl-microsat.upd.edu.ph/diwata2>
- [6] Automatic Packet Reporting System (APRS), 2002, [www.aprs.org](http://www.aprs.org)
- [7] R.J. Twiggs, H. Heidt, J. Puig-Suari, A.S. Moore, S. Nakasuka, *A CubeSat: a new generation of Picosatellite for education and industry low-cost space experimentation*, Proceedings of the 14th Annual AIAA/USU Conference on Small Satellites, August, 2000.
- [8] PSAT2 - Amateur Radio Communications Transponders, <http://aprs.org/psat2.html>

- [9] A. Addaim, A. Kherras, Z. Gennoun, *Design of WSN with Relay Nodes Connected Directly with a LEO Nanosatellite*, Int. J. of Computer and Communications Engineering, **3**(5), 310-316, 2014.
- [10] H. Bedon, C. Miguel, A. Fernandez, J.S. Park, *A DTN System for Nanosatellite-based Sensor Networks using a New ALOHA Multiple Access with Gateway Priority*, Smart Computing Review, **3**(5), 383-396, 2013.
- [11] M. De Sanctis, E. Cianca, G. Araniti, et. al., *Satellite Communications Supporting Internet of Remote Things*, IEEE Internet of Things Journal, **3**(1), 113-123, 2016.
- [12] J. Guzman, G. Comina, H. Bedon, et. al., *Global water pollution monitoring using a nanosatellite constellation - Novel Ideas for Nanosatellite Constellation Missions Edition 1*, International Academy of Astronautics, 2012.
- [13] A. Addaim, E.B. Zantou, A. Kherras, *Design and Analysis of Store-and-Forward Data Collection Network using Low-cost LEO Small Satellite and Intelligent Terminals*, Journal of Aerospace Computing, Information, and Communication, **5**, 35-46, 2008.
- [14] A. Addaim, E.B. Zantou, A. Kherras, *DSP implementation of integrated store-and-forward APRS payload and OBDH subsystems for low-cost small satellite*, Aerospace Science and Technology, **12**(4), 308-317, 2008.
- [15] A. Addaim, A. Kherras, Z. Guennoun, *Enhanced MAC protocol for designing a wireless sensor network based on a single LEO Picosatellite*, Int. J. of Sensor Networks, **23**(3), 143-154, 2017.
- [16] G. Ridolfi, S. Corpino, F. Stesina, et. al., *Constellation of CubeSats: 3-Star in the HUMSAT/GEOID Mission*, Proceedings of the 62nd International Astronautical Congress (IAC), October, 2011.
- [17] Q. Verspiepren, T. Obata, S. Nakasuka, *Innovative Approach to Data Gathering in Remote Areas Using Constellations of Store & Forward Communications Cubesats*, Proceedings of the 31st International Symposium on Space and Technology (ISTS), June, 2017.
- [18] M.G. Jenkins, J.C. Alvarado, A.J. Calvo, A.C. Jimenez, et. al., *Project Irazu: Advances of a Store & Forward CubeSat Mission for Environmental Monitoring in Costa Rica*, Proceedings of the 68th International Astronautical Congress (IAC), September, 2017.
- [19] A.C. Salces, S.B.M. Zaki, S. Kim, H. Masui, M. Cho, *Project Irazu: Design, Development, Testing and On-Orbit Performance Results of a Low-cost Store-and-Forward Payload Onboard a 1U CubeSat Constellation for Remote Data Collection Applications*, Proceedings of the 69th International Astronautical Congress (IAC), October, 2018.
- [20] E.B. Zantou, A. Kherras, *Small Mobile Ground Terminal Design for a Microsatellite Data Collection System*, Journal of Aerospace Computing, Information, and Communication, **1**, 364-371, 2004.
- [21] E.B. Zantou, A. Kherras, A. Addaim, *Performance Evaluation of a Single Microsatellite Data Collection System using Small Ground Terminals*, Journal of Aerospace Computing, Information, and Communication, **3**, 63-72, 2006.
- [22] W.A. Beech, D.E. Nielsen, J. Taylor, AX.25 Link Access Protocol for Amateur Packet Radio Version 2.2, Tucson Amateur Packet Radio Corporation, 1997, <https://www.tapr.org/pdf/AX25.2.2.pdf>
- [23] Nagai Giken, Types, characteristics, terms, etc. of steel (metal materials) stipulated by JIS, 2018, [https://www.hamadashokai.co.jp/goods/detail.php?match\\_code=4906365066865](https://www.hamadashokai.co.jp/goods/detail.php?match_code=4906365066865)
- [24] Hamadashokai Co., Ltd., GOHSEN PE Hunter Lock (100 m connection), 2018, <http://www.nagai-giken.com/snonfm18.html>
- [25] S.B.M. Zaki, M.H. Azami, T. Yamauchi, S. Kim, H. Masui, M. Cho, *Design, Analysis and Testing of Monopole Antenna Deployment Mechanism for BIRDS-2 CubeSat Applications*, Proceedings of the 1st International Conference on Space Weather and Satellite Application, August, 2018.
- [26] J.A. King, AMSAT/IARU Annotated Link Model System Version 2.4.1, 22 October 2006, <https://amsat-uk.org/tag/link-budget/>
- [27] M2 Antenna Systems Inc., EB-144/RK-2M, 2018, <http://www.m2inc.com/amateur/eb-144-rk-2m-135-150-mhz/>